THE PREDICTION OF THE DISCHARGE COEFFICIENT OF A PIANO KEY WEIR COMPARED TO A LABYRINTH WEIR

HAMK
HÄMEEN AMMATTIKORKEAKOULU
HÄME UNIVERSITY OF APPLIED SCIENCES

Bachelor's thesis

Hämeenlinna University Centre

Degree Programme in Construction Engineering

Spring 2021

Quoc Vinh Vuong

HÄMEEN AMMATTIKORKEAKOULU
HÄME UNIVERSITY OF APPLIED SCIENCES

Degree Programme in Construction Engineering
Hämeenlinna University Centre

Author Quoc Vinh Vuong **Year** 2021

Subject The prediction of the Discharge Coefficient of a Piano Key Weir compared to a Labyrinth Weir.

Supervisors Andrew K. Petersen, Stephen Mai (HS Mainz)
Niina Kovanen (process in HAMK)

ABSTRACT

Weirs are free-surface hydraulic structures built across open channels, such as rivers or lakes, to control the upstream flow of water. As they are passive hydraulic control barriers, it is critical to understand how the geometry specifications and discharge efficiency contribute to the sufficiency and safety of a weir's operation.

A Labyrinth Weir is a non-linear weir which has been configurated in a zigzag geometry with increase in weir length within a fixed channel width. A Piano Key (PK) Weir, developed as an alternative for a traditional Labyrinth Weir, is another type of non-linear weir used particularly for free-surface flow control structures with relatively small channel footprints. Non-linear weirs are used rather than linear weirs due to their significant increase in discharge efficiency within the restricted channel and spillway footprints.

To have a better understanding of the effects of different weir geometries on discharge efficiency, a laboratory-scale, 2-cycle Trapezoidal Labyrinth (TL) Weir, in both aerated and unaerated situations, were tested. Hypothetical data of a laboratory-scale, 2-cycle PK Weir were also predicted based on the physical model of hydraulics. As a result, the influence of the following PK and TL Weir's geometries/modifications were recognized: TL Weir with normal and inverse orientation, PK Weir with and without ramps, both on the inlet and outlet keys. Based on the experimental and hypothetical results, the discharge coefficient and head-discharge relationships were evaluated.

Previous research has found that the discharge rate of PK Weirs can be four times higher than TL Weirs. However, in this research, it was found that PK Weirs are from 23% to 135% more efficient in discharge efficiency compared to TL Weirs.

Keywords Discharge Coefficient, Discharge Efficiency, Piano Key Weir, Trapezoidal Labyrinth Weir, Rectangular Labyrinth Weir, Fluid Mechanics

Pages 52 pages

ACKNOWLEDGEMENTS

Firstly, I would like to thank Professor Mai for introducing the thesis topic and for his answers to all my uncertainties. Thank you, Professor Petersen, for providing me the opportunity to be involved in this research, for your hours of guidance given and for your patient support, mentally and professionally while conducting this research.

Secondly, I would like to send my gratitude to my classmate - Mr. Emmanuel Possible Businge for his previous informative research, professionally, and his helpful advice, suggestions, and answers to all my questions, personally. Thank you, Mr. Erich Weiler, for the photos of the weirs, the testing equipment, and the experimental setup of the hydraulic laboratory in Hochschule Mainz University of Applied Sciences. Thank you, Mr. Carsten Mahnel, for showing me the hydraulic laboratory and providing me literature to begin with.

Thirdly, I would also like to thank my host university Hochschule Mainz University of Applied Sciences in Germany, my home university Häme University of Applied Sciences (HAMK) in Finland and Erasmus+ Programme for facilitating me the opportunity to study exchange and to complete my thesis even during the pandemic Corona Virus Covid-19.

Finally, I give special thanks to my family, friends and classmates for their moral support and encouragement. Without them, I could have never had studied abroad in Finland, Germany and above all, complete my final thesis and the bachelor's degree.

Quoc Vinh Vuong

CONTENTS

LIST OF FIGURES / GRAPHS / TABLES

Figure / Graph / Table Page

LIST OF SYMBOLS

Symbol	Definition	Unit
α	angle	°
B	control structure footprint length	m
B_o	upstream or outlet cycle cantilever length	mm
B_i	downstream or inlet cycle cantilever length	mm
C_d	discharge coefficient	
g	acceleration of gravity = 9.81	m/s^2
H	piezometric head	mm
H_t	total head (piezometric head plus velocity load)	mm
L	weir length	mm
N	number of weir cycles	
P	weir height	mm
Q	discharge	l/s
T_s	wall thickness	mm
V	velocity	m/s
W	width of weir	mm
W_i	inlet cycle width	mm
W_o	outlet cycle width	mm
w	cycle width	mm

GLOSSARY OF TERMS

Terminology	**Definition/Comment**
Dam	Structure built across a stream, a river, or an estuary to retain water.
Spillway	Passage for surplus water over or around a dam when the reservoir itself is full.
Crest	The bottom edge over which the water flows.
Nappe	The sheet of water which springs free from the crest.
Discharge Efficiency	The increase in discharge efficiency means that less reservoir storage needs to be reserved for flood routing (increased water storage) without compromising dam safety.

1 INTRODUCTION

This thesis was done during the exchange period in Hochschule Mainz University of Applied Sciences but accepted as part of HAMK-degree.

This chapter introduces the background to the research problem with particular respect to the Discharge Coefficient of a Piano Key Weir compared to a Trapezoidal Labyrinth Weir. The aims and objectives of the research along with the scope and limitations of the research are stated. The structure of the thesis is also explained.

1.1 Background

Weirs are hydraulic structures, barriers built across open channels, such as rivers or lakes, to control the upstream flow of water (Hillhouse, 2019). Weirs are used not only to measure and adjust the water level to control flooding, generate power, improve navigation of water but also to act as spillways for dams (Hanania, Stenhouse and Donev, 2017). There are two types of spillways: free-flow spillways and gated ones. Weirs are free-flow spillways, they are simpler and safer than the gated ones, according to Lemperiere and Ouamane (2003).

Weirs are also called small dams where the major difference between the two structures is: the purpose of building dams is to create reservoir and water storage while the construction of weirs is not for storing but controlling (Hanania et al., 2017).

Figure 1. Bedford Weir in Queensland, Australia (Queensland, 2020)

Figure 2. Systems of weirs below Shinner's Bridge
(Wikipedia Commons, 2020)

As a weir is a passive hydraulic control barrier, discharge efficiency and geometry specifications are the most critical factors contributing to the sufficiency and safety of a weir's operation. There are several types of weirs depending on the shape of the crests such as sharp-crested weirs, broad-crested weir, Ogee weir. They can be classified as rectangular, triangular, trapezoidal, v-notch, based on the geometry of the openings.

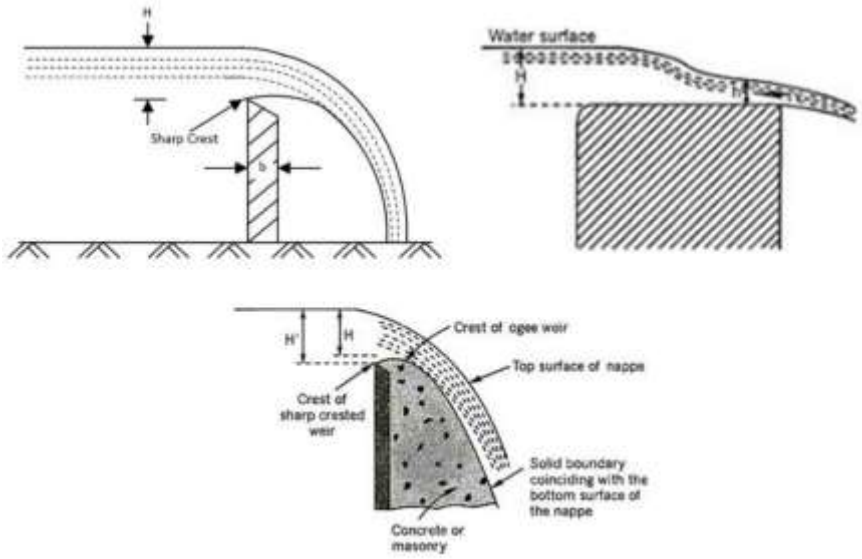

Figure 3. Illustrations of a sharp-crested weir (left), a broad-crested weir (right) and an Ogee weir (bottom) (Engineering Notes, 2020)

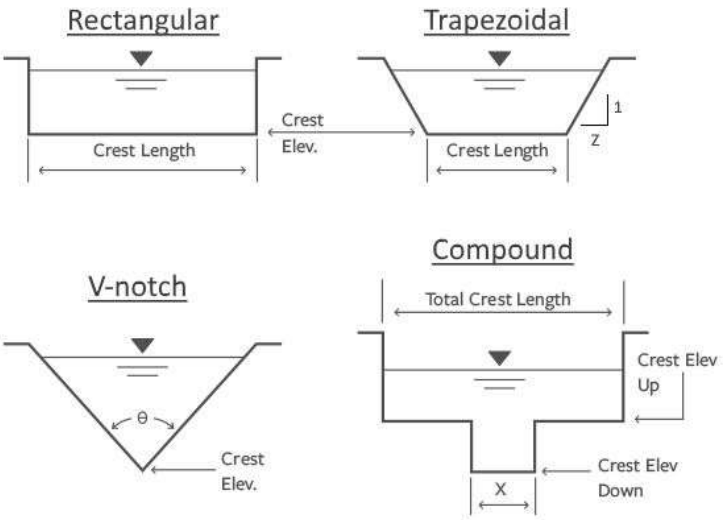

Figure 4. Illustrations of different weir classifications according to their openings (Engineering Notes, 2020)

This Research focuses on two types of weirs, a Piano Key (PK) Weir and a Trapezoidal Labyrinth (TL) Weir. Hillhouse (2019), cited by Businge (2020), stated that "A Labyrinth Weir is a structure designed to convey large flows at low heads by increasing the effective length of the weir crest with respect to the channel breadth." (p.1).

Furthermore, a Labyrinth Weir, shown in Figure 7 (A), is a non-linear weir which has been orientated in a zigzag configuration with increased weir length L in a fixed channel width W (Anderson, 2011). With that modification in geometry, the discharge efficiency in Labyrinth Weir can be increased by 3 to 4 times compared to a Linear Weir (Tullis, Amanian and Waldron, 1995).

Figure 5. Photo of the Trapezoidal Labyrinth Weir in Lake Townsend dam, Greensboro, North Carolina, USA (Schnabel Engineering, 2020)

For some spillway designs, some of the benefits of the Labyrinth Weir are lost due to the limited channel width (W) and control structure footprint length (B), as seen in Figure 5. Moreover, PK Weir has smaller foundation footprint than Labyrinth Weir due to their cantilevered apex geometry (Paxson, Tullis and Hertel, 2014). Therefore, a PK Weir is developed as an alternative for a traditional Labyrinth Weir, particularly for smaller control structure footprint applications (Anderson, 2011). The discharge rate of PK Weirs can be increased by four times (Lemperiere and Ouamane, 2003).

Figure 6. Photo of a PK Weir of Gloriettes dam in France (Schleiss, 2011)

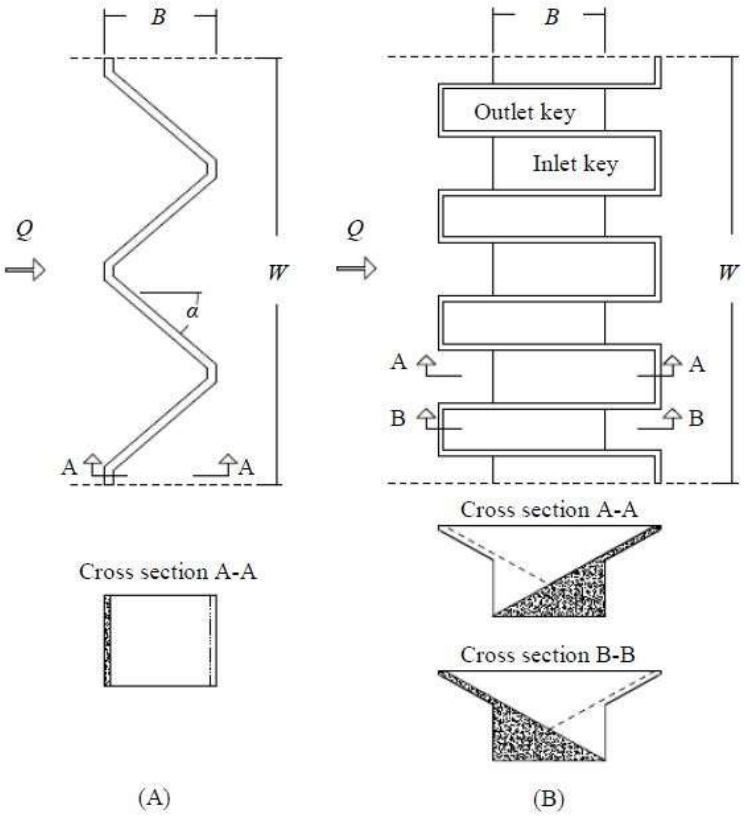

Figure 7. Drawings of a TL Weir (A) and a PK Weir (B) (Anderson, 2011)

The discharge coefficients of weirs can be determined using either the Poleni (Eq. 1) or Weisbach equation (Eq. 2) (Hamburg University of Technology, 2020).

$$Q = \frac{2}{3} \times C_d \times L \times \sqrt{2g \times H_t{}^3} \quad (1)$$

The Poleni original equation can be simplified as in Eq. 1a below:

$$Q = \frac{2}{3} \times C_d \times L \times \sqrt{2g} \times H_t{}^{\frac{3}{2}} \quad (1a)$$

where Q is the discharge, C_d is the discharge coefficient, g is the gravitational constant, L is the crest length, H is the piezometric head, H_t is the total upstream head measured relative to the weir crest plus velocity head $\frac{V^2}{2g}$.

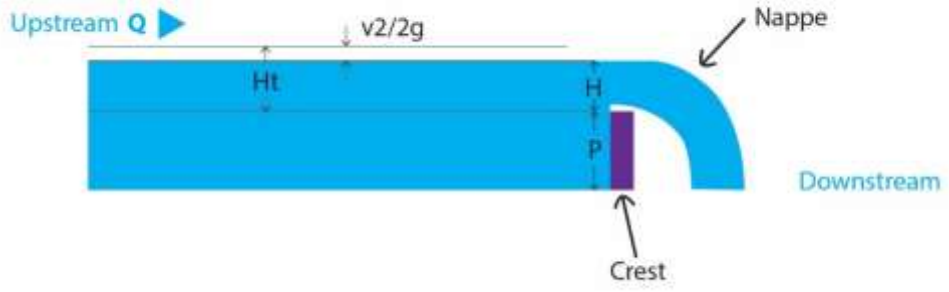

Figure 8. Weir Parameters on a Sharp-Crested Linear Weir
(The Author, 2020)

The Weisbach equation is as follows:

$$Q = \frac{2}{3} \times C_d \times L \times \sqrt{2g} \times [\left(H + \frac{V^2}{2g}\right)^{\frac{3}{2}} - \left(\frac{V^2}{2g}\right)^{\frac{3}{2}}] \quad (2)$$

Geometries play an important role in increasing or decreasing the discharge efficiency of free-flow weirs. There are three ways to increase the discharge efficiency of a weir: (1) increasing the width W of the weir, (2) lowering the weir height P and/or (3) increase length of the weir structure L within the existing channel width by replacing a linear weir with a non-linear weir (Anderson, 2011).

To have a better understanding of the differences of head-discharge relationships, this research compares the discharge coefficient of scale models of a PK Weir and a TL Weir. The comparison is made by predicting the outcome of a laboratory experiment using one scaled model of a PK Weir and comparing the findings to the previous experiment using one scaled model of a TL Weir (Businge, 2020).

1.2 Motivation for the Research

The reasons for developing the research question are:

- Compare the Discharge Coefficient of a PK Weir to that of a TL Weir under similar flow conditions.
- Compare the results of this research with a similar and already completed experiment.

Research Aim and Objectives

Against the background outlined earlier, this research project is undertaken with the aim of Predicting the Discharge Coefficient of a scaled model PK Weir from hypothetical data and comparing it with a scaled TL Weir. To achieve this aim, the following objectives are pursued:

Objective #1 - Understand the literature, methodology and findings of the previous study (Businge, 2020).
Objective #2 - Adapt the methodology for collecting hypothetical data.
Objective #3 - Predict from the hypothetical data the Discharge Coefficient of a PK Weir and compare to the collected data from the laboratory experiment of a TL Weir.
Objective #4 - Discuss the results of the analysis/comparison.
Objective #5 - Ensure the next researcher will be able to conduct the actual laboratory experiment described in this study.

1.3 Scope of the Research

The study is limited to one physical scaled model of a PK Weir and one physical scaled model of a TL Weir.

1.4 **Chapter Summary**

This chapter has introduced the background and the need to conduct a laboratory experiment to determine the Discharge Coefficient of a PK Weir and compare to that of a TL Weir. The aim and objectives of the research have been stated and the scope and limitations of the research given. The structure of the report has also been explained.

The chapter has demonstrated that there is a clear need to understand the literature, methodology and findings of a previous study of the Discharge Coefficient of a Labyrinth Weir (Businge, 2020). Due to the novel Corona Virus Covid-19 (HS Mainz, HAMK, 2020) Laboratory Work by the Researcher was not possible. Therefore, the methodology of the previous study has been adapted to predict from hypothetical data the Discharge Coefficient of a PK Weir and compare to laboratory data from the experiment previously performed using a TL Weir. The prediction is discussed with the aim that the next researcher will be able to conduct the actual laboratory experiment described in this thesis.

The next chapter will review the extant literature.

2 LITERATURE REVIEW

This chapter presents and critiques the literature in the extant body of knowledge.

2.1 Overview

A study by Anderson (2011) represents significant literature in the field and it describes sets of experiments conducted on the head-discharge relationships of different types of PK Weirs and TL Weirs.

2.2 Place and Publication of the Significant Literature

The research by Anderson (2011) was conducted at the Utah Water Research Laboratory, located in Utah State University, Logan, Utah, the United States of America.

2.3 Methodology used in the Significant Literature

2.3.1 Methodology used by Anderson (2011)

The methodology used can be adapted for this research because:

- Anderson (2011) used scaled models of PK Weirs and TL Weirs.
- All the necessary equipment used to conduct the research were available at the Hydraulic Laboratory of Hochschule Mainz University of Applied Sciences. A similar approach would therefore be possible.

The researcher in the found research had many different experiments with many PK Weirs and Labyrinth Weirs with different configurations (Figure 9). A list of experiments in the research of Anderson (2011) are as follows:

- Comparisons of discharge Q and total head H_t between different types of PK Weirs.
- Comparisons of discharge coefficient C_d and ratio total head over weir height H_t/P between different types of PK Weirs.
- Comparisons of discharge coefficient C_d and ratio total head over weir height H_t/P between different types of additional features such as sloped floors, fillets, raised crests, crest types.
- Discharge efficiency comparisons with multiple geometric configurations.
- Comparisons of discharge coefficient C_d and ratio total head over weir height H_t/P between 7 different types of TL Weir and one type of PK Weir.

Weir	Abbreviation
PK weir with $W_i/W_o = 1.5$	$PK_{1.5}$
PK weir with $W_i/W_o = 1.25$ [recommended design by Lempérière (2009)]	$PK_{1.25}$
PK weir with $W_i/W_o = 1$	$PK_{1.0}$
PK weir with $W_i/W_o = 0.8$	$PK_{0.8}$
PK weir with $W_i/W_o = 0.67$	$PK_{0.67}$
PK weir with parapet wall	PKR
PK weir with fillets	PKF
PK weir with raised crest, fillets, and flat top crest type	PKRFF
PK weir with raised crest, fillets, and half round crest type	PKRFH
Rectangular labyrinth weir with no sloped floors	RL
Rectangular labyrinth weir with sloped floors in inlet and outlet cycles	RLRIO
Rectangular labyrinth weir with sloped floors in inlet cycles	RLRI
Rectangular labyrinth weir with sloped floors in outlet cycles	RLRO

Figure 9. Testing matrix of the research by Anderson (2011), not including other types of TL Weirs (with different angles)

2.3.2 Differences between the Significant Research and this Research

- The flume used by Anderson (2011) was 7.30 m long, 0.93 m wide, 0.60 m deep while in this research it was 10 m long, 0.30 m wide and 0.47 m deep.
- The research by Anderson (2011) used one pump capable of 240.70 l/s while this research used one pump with a maximum capacity of 21 l/s.
- In the research by Anderson (2011), tests were run with flows ranging from 7.08 l/s to 240.70 l/s while in this research, the flows were from 1 l/s to 21 l/s.
- The PK Weirs in Anderson's research (2011) were designed as 4 cycles while in this research, the weirs are designed as 2 cycles.
- The Labyrinth Weirs in Anderson's research (2011) were designed as 4 cycles while in this research, the weirs are designed as 2 cycles.
- The research by Anderson (2011) had one PK Weir and 7 TL Weirs with different configurations while the current research had/has only one model of PK Weir and one model of TL Weir in the same experimental comparison.
- In the research by Anderson (2011), the researcher experimented 3 different type of Rectangular Labyrinth Weirs: Rectangular Labyrinth Weir (RL), Rectangular Labyrinth Weir with ramps in outlet keys (RLRO) and Rectangular Labyrinth Weir with ramps in inlet keys (RLRI). This research used similar types of weirs but different in naming system, PK Weir rather than Rectangular Weir.

2.3.3 The Weaknesses in the Research of Anderson (2011)

The weaknesses found in the research by Anderson (2011) that have been strengthened in this research are:

- In Anderson's research (2011), a rolling point gauge (readability of 0.0005-ft – 0.1524 mm) instrumentation carriage were used to measure the nappe height and water depth in various locations while in this research, the sophisticated-level-wave-measurement device UltraLab ULS HF54/58 was used.
- The research by Anderson (2011) did not mention the Labyrinth Weir's orientation and therefore an assumption was made that the found research used normal Labyrinth Weir orientation while in this research, both orientations (normal as M-shape and inverse as W-shape) were tested. The weir orientation will be explained in chapter 2.4.3 below.

2.3.4 Results of the Research of Anderson (2011)

Results of the discharge coefficients C_d versus total head over weir height ratio H_t/P were plotted in Figure 10 and 11 by Anderson (2011).

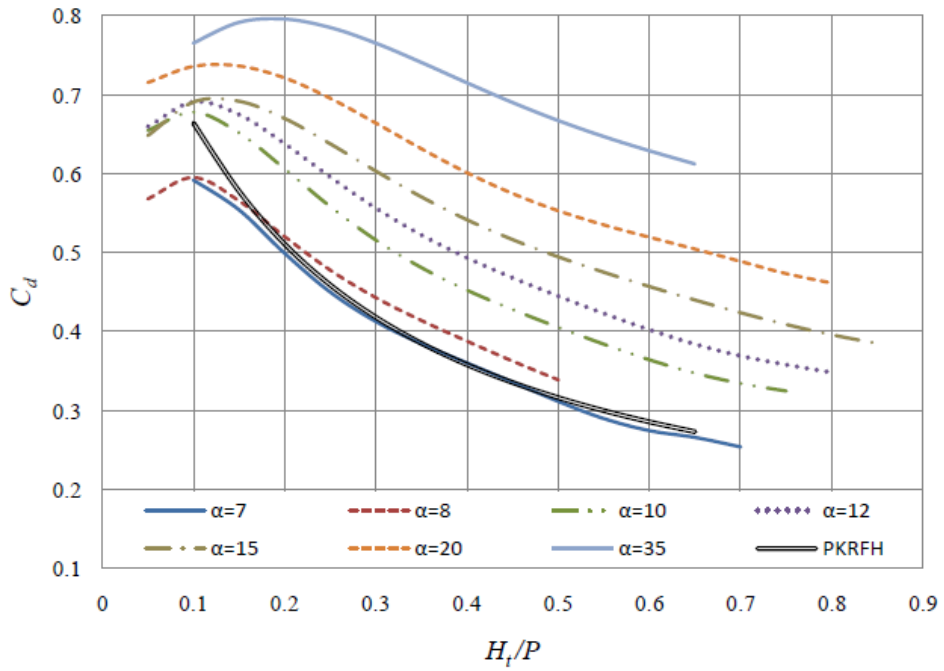

Figure 10. C_d vs. H_t/P data for TL Weirs of various α and PKRFH (PK Weir with raised crest, fillets, and half round crest type) (Anderson, 2011)

As seen in Figure 10, discharge per unit weir length (C_d) of Labyrinth Weir decreases when the sidewall angle (a) decreases. A PK Weir is similar to a Labyrinth Weir with a = 0° (Anderson, 2011). Therefore, PKRFH's C_d curve is more consistent to Labyrinth Weir's with smaller angles such as a = 7° and a = 8°. Moreover, PK Weir has smaller C_d than most of Labyrinth Weir's, specifically with a > 7°.

In general, the curve of Labyrinth Weir increases to a specific point then decreases while PK Weir has a distinctive decreasing curve since beginning. The graph of Labyrinth Weir a = 20° and the graph of PKRFH from the research of Anderson (2011) will be used to compare with the results from this experiment, which as similar scaled models Labyrinth Weir of a = 19.1° and PK Weir a = 0°.

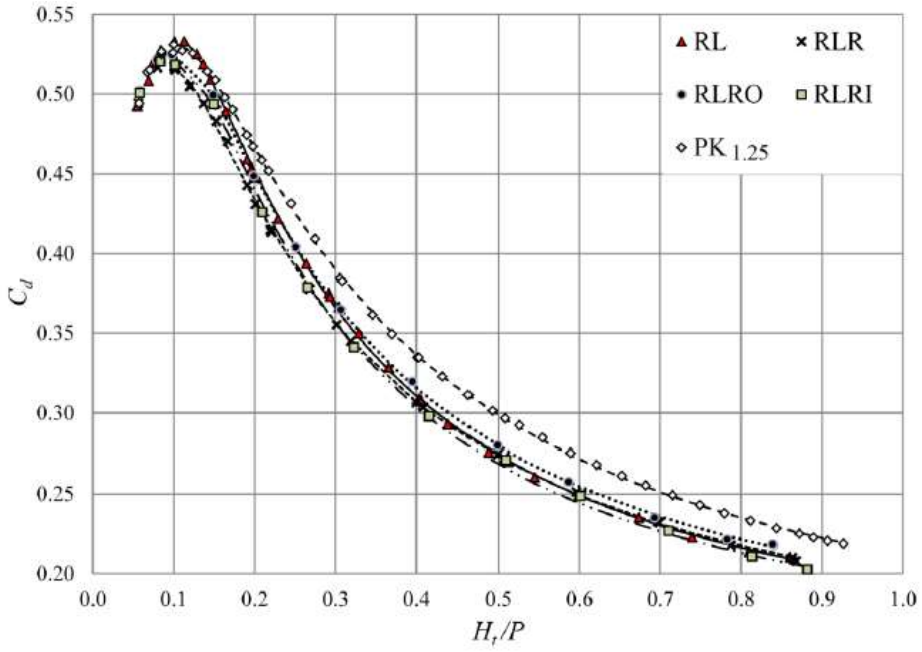

Figure 11. C_d vs. Ht/P data for several types of Rectangular Labyrinth Weirs (RL, RLRO, RLRI, RLR) and one type of PK Weir (PK $_{1,25}$) (Anderson, 2011)

In this research, PK Weir will be comparable with RL Weir in Anderson's research (2011). As seen in Figure 11, RL Weirs have the same curve trend as TL Weir (in Figure 10) as increasing to a specific point then decreasing. The difference is Rectangular Labyrinth Weir's curve tends to decrease more than that of TL Weir's. There is not such a big difference between multiple types of RL Weirs, with or without ramps.

The simplified and combined graph of Rectangular Labyrinth Weir with ramps in outlet keys RLRO, Rectangular Labyrinth Weir with ramps in inlet keys RLRI, Rectangular Labyrinth Weir RL and TLW a = 20° were plotted in Figure 12 (The Author, 2020). This graph will be compared with the graph from this experiment in Chapter 5.

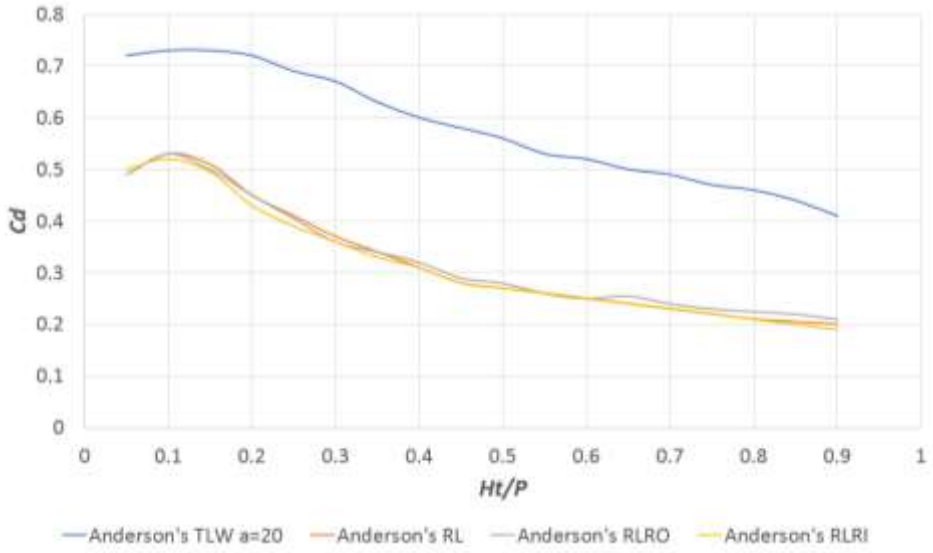

Figure 12. A graph of Rectangular Labyrinth Weir with ramps in outlet keys RLRO, Rectangular Labyrinth Weir with ramps in inlet keys RLRI, Rectangular Labyrinth Weir RL and Trapezoidal Labyrinth Weir TLW α=20° (Anderson, 2011)

2.4 **Other Relevant Findings from Other Researchers**

2.4.1 Literature on the Different Types of PK Weirs

Schleiss (2011) cited Lemperiere and Ouamane, (2003) about two main developed types of PK Weirs, Type-A and Type-B as shown in Figure 13.

Type-A (A): Features both upstream and downstream cantilever cycles (B_i/B_o = 1 typically) (Anderson, 2011). This type of PK Weir may be used for discharges up to 20 m^3/s (20,000 l/s) and preferably made using precast concrete elements. A foundation with small footprint allows placing this configuration on existing gravity dam crests to increase the flood release capacity.

Type-B (B): Features longer upstream cantilever cycles ($B_i + B_o$ = constant typically) and no downstream cantilever cycles (B_i/B_o = 0) (Anderson, 2011). This configuration is attractive for new dam projects due to lesser structural loads with high discharges. Discharges up to 100 m^3/s (100,000 l/s) are possible.

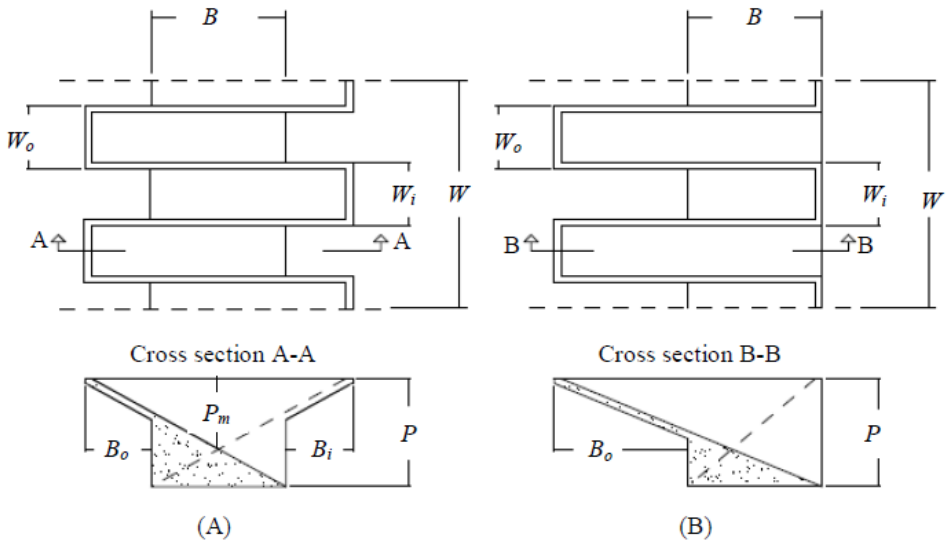

Figure 13. PK Weir Type-A (A) and Type-B (B) Geometric Parameters (Anderson, 2011)

Many additional features have been developed and added to the existing configuration with the purpose to increase the discharge efficiency as well as lower the cost while maintaining the safety issues (Schleiss, 2011; Anderson, 2011) such as: parapet walls, fillets, different crest type.

Parapet walls are vertical walls placed on top of the crest of the conventional PK Weir, transforming its upper part to a rectangular labyrinth weir (Schleiss, 2011). The total weir height is increased without increasing the length of the cantilevers. Study by Ribeiro et al. (2009) found that there was a 15% increase in discharge efficiency when increasing the total PK Weir height by 12.3% with the additional parapet walls.

Machiels, Erpicum, Archambeau, Dewals and Pirotton (2012) acknowledged that it is more convenient and cost-effective to use standard (without parapet walls) PK Weir. Research by Machiels et al. (2012) found that the discharge capacity does not increase when parapet walls are placed on a PK Weir having an optimal weir height already. Results also show that the discharge capacity does not change for PK Weirs having the same total height, with or without parapet walls. The researchers concluded that adding parapet walls is efficient only when the total weir height is not optimal yet and PK Weir with parapet walls can be used for new rehabilitations.

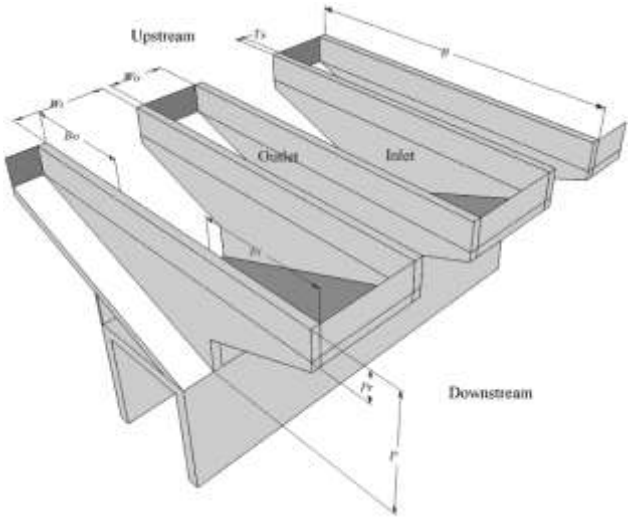

Figure 14. Illustration of a PK Weir with additional parapet walls (Machiels et al. 2012)

Sidewall angle is among many optional features that have been developed for PK Weir. A sidewall angle is built to narrow the inlet key and widen the outlet key. Discharge capacity is likely improved (Schleiss, 2011).

Lemperiere and Ouamane (2003) and Ouamane and Lemperiere (2006) reported that there were increases of 10% and 7%, respectively, in discharge efficiency when using fillets (e.g. triangular, rounded, etc.) under the upstream overhangs. Studies have also shown the improved hydraulic shapes when PK Weir featuring fillets.

Figure 15. A model of PK Weir with Round Fillets in the upstream overhangs, Raised Crest (Parapet Walls) and Half Round Crest (Anderson, 2011)

Anderson (2011) found out that in Barcouda et.al. (2006) and Ribeiro, Boillat, Schleiss, Laugier and Albalat's studies (2007) the crest shape (e.g.,

flat crest, half round crest, etc.) has affected the discharge efficiency. Barcouda et al. (2006) and Riberio et al. (2007) experimented three different PK Weir crest geometries: an upstream quarter round, a downstream quarter round and a flat crest. Results showed that upstream quarter round is the most efficient among the three. However, discharge efficiency relative change, particular to each crest shape, was not recognized.

2.4.2 Literature on Vented and Unvented Overflow

Insufficient aeration or non-aeration, whether by poor sidewall geometry or insufficient vertical drop from the weir crest to the downstream water surface can increase discharge by as much as 25%, resulting in flow readings that are dramatically different than would otherwise be obtained by an aerated weir nappe. To avoid the nappe collapses against the face of the weir, air must be allowed to replenish that which is entrained by the nappe. In other words, weir should be vented or aerated (Open Channel Flow, 2020).

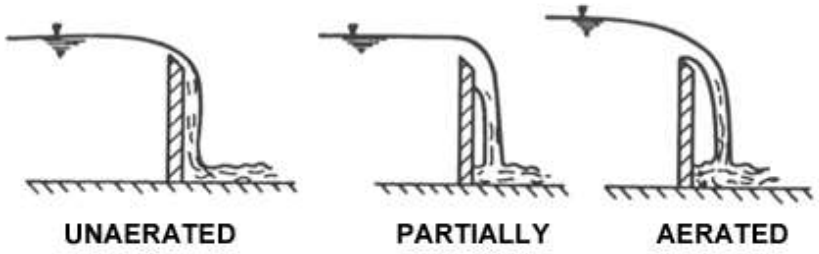

Figure 16. Illustrations of unaerated, partially aerated, and aerated situations (Open Channel Flow, 2020)

Study by Young (2018) showed that nappe behavior is classified depending on the weir type. With Labyrinth Weirs, study recognized four types of nappe behavior: clinging, aerated, partially aerated, and drowned. For PK Weir models, five nappe behaviors were observed: clinging, partially clinging, aerated, partially aerated, and drowned.

Aerated refers to a detached nappe with an air cavity between the nappe and the weir crest. Partially aerated indicates a non-uniform and unstable air cavity. Drowned (unaerated) describes a thick nappe without an air cavity, as shown in Figure 16. Clinging refers to flow adhering to the downstream wall of the weir, as in Figure 17. Finally, partially clinging refers to the stable nappe condition where water clings to the downstream sloped wall yet detaches from the vertical side walls near the sharp corners (Young, 2018).

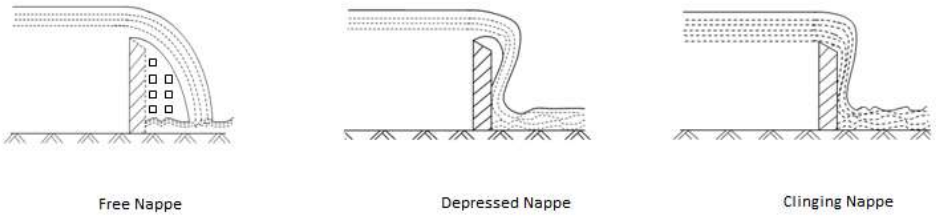

Figure 17. Different kinds of nappe behavior (Codecogs, 2020)

Truong, Ho and Dinh (2006) found that, in general, PK Weirs are better at nappe aeration than TL Weirs due to their cantilever (or overhang) configurations.

2.4.3 Literature on the effect of weir orientation of Labyrinth Weirs

Experiments on the effect of normal and inverse orientation of Labyrinth Weirs were done by Idrees, Al-Ameri and Das (2016) who concluded that weir orientation does not significantly affect the Discharge Efficiency and Discharge Coefficient, as seen in Figure 16. In the study by Idrees et al. (2016), the normal orientation was W-shape Labyrinth Weir and the inverse orientation was M-shape. In the contrary, the normal orientation was M-shape Labyrinth Weir and the inverse orientation was W-shape Labyrinth Weir in Businge's study (2020).

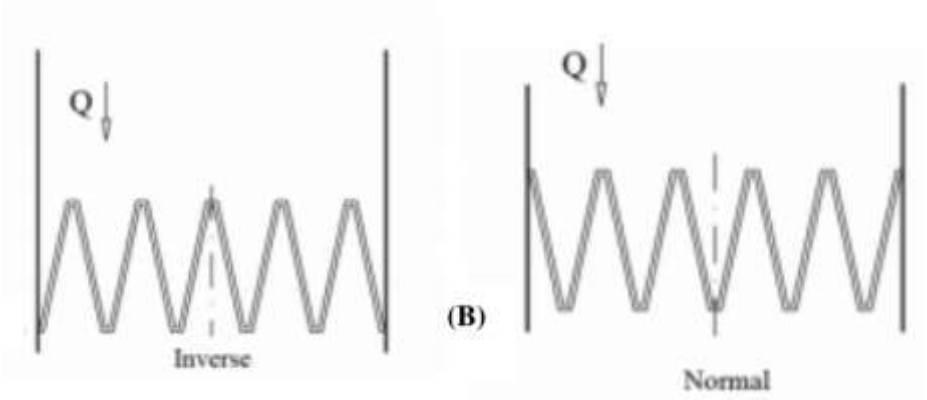

Figure 18. Labyrinth Weir Orientations (Idrees, Al-Ameri and Das, 2016)

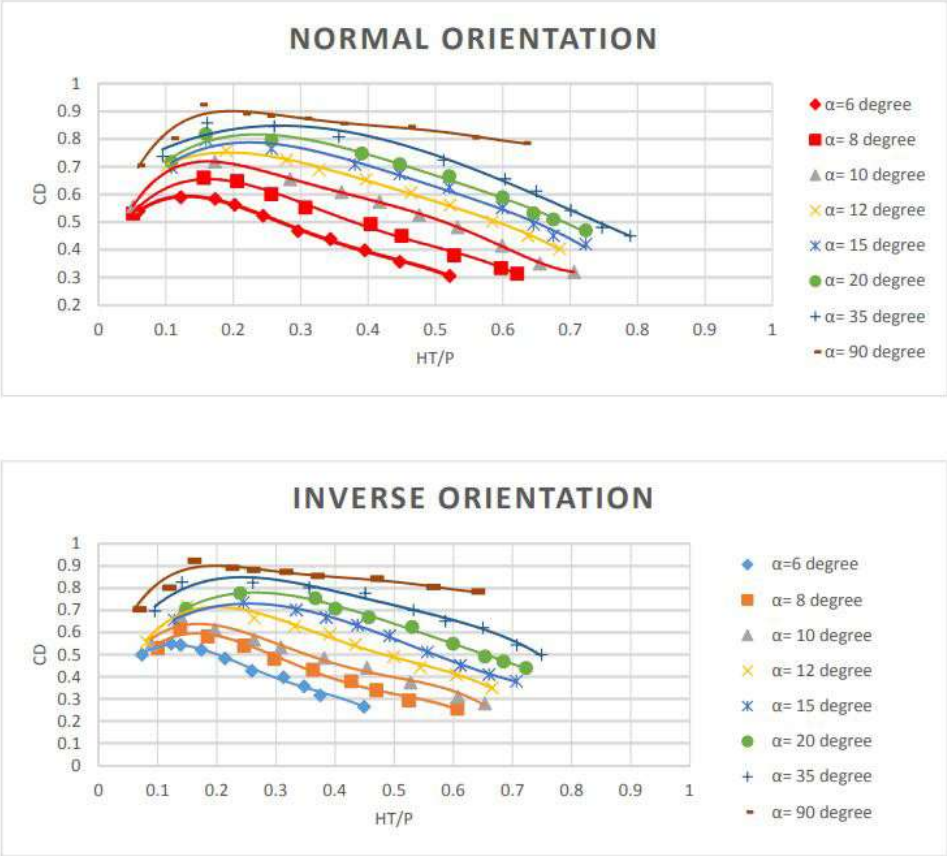

Figure 19. Comparison C_d versus H_t/P values between normal and inverse Labyrinth Weirs (Idrees, Al-Ameri and Das, 2016)

A similar conclusion was drawn in the laboratory experiments of Businge (2020). This research considers both findings by conducting testing experiments with both normal and inverse orientation of Labyrinth Weirs to find out whether a similar conclusion can be made.

2.4.4 Literature on the cost comparison between PK Weir and Labyrinth Weir

PK Weirs and Labyrinth Weirs are both folded in plan to increase the discharge capacity within a given channel width. Due to their cantilevered overhangs as seen in Figure 6, PK Weirs have smaller foundation footprint than Labyrinth Weirs. Therefore, when limited footprint is applicable, using PK Weirs is more practical and economical (Paxson, Tullis and Hertel, 2014).

Study by Paxson et. al. (2014) compared the construction cost of a PK Weir and a Labyrinth Weir. The configurations of weirs were as follows:

- PK Weir: 4 cycles, total spillway width W = 14.2 m, total weir length L = 72.3 m, total upstream to downstream footprint B_t = 7.4m and base B = 3.8 m.

- Labyrinth Weir: 2 cycles Trapezoidal type, sidewall angle a = 15°, total spillway width W = 14.1 m, total weir length L = 44.8 m and total upstream to downstream footprint B = 10.8 m.
- Both weirs had the same height P = 3 m and similar head-discharge relationships. Computed discharge for a design head H_t = 2.4 m was 186 m^3/s = 186000 L/s. The training walls were 5.4 m.

Table 1. PK weir quantity and cost estimate (concrete only)

Element	Type of Concrete	Volume m^3	Unit Cost USA$/$m^3$	Total Cost USA$
Base	Mass	56.5	$250	$14,125
Weir Walls	Reinforced	11.5	$800	$9,200
Overhangs	Reinforced	6.4	$800	$5,120
Training Walls	Reinforced	35.0	$700	$24,500
Slab	Reinforced	15.8	$300	$4,740
Total		125		$57,685

Table 2. Labyrinth weir quantity and cost estimate (concrete only)

Element	Type of Concrete	Volume m^3	Unit Cost USA$/$m^3$	Total Cost USA$
Weir Walls	Reinforced	50.4	$800	$40,320
Training Walls	Reinforced	50.8	$700	$35,560
Slab	Reinforced	86.9	$300	$26,070
Total		188		$101,950

Figure 20. Construction volume and cost comparison between a PK Weir and a Labyrinth Weir in terms of concrete material only, unit cost in US$/$m^3$ (Paxson, Tullis and Hertel, 2014)

As seen in Figure 20, with similar head-discharge relationships, PK Weir's total concrete volume was 35% less than that of Labyrinth Weir and therefore, the cost was estimated 45% less than Labyrinth Weir's. This is because PK Weir has reduced foundation (base) with the same width B (check Figure 7).

Table 3. Labyrinth and PK weir concrete volumes and costs for fixed channel dimensions

Spillway	Concrete Volume m^3	Total Cost USA$
PK Weir	212	$90,075
Labyrinth Weir	188	$101,950

Figure 21. Estimated concrete volumes and costs of PK Weir and Labyrinth Weir with fixed channel dimensions, assuming the concrete volumes for the slab and training walls for the PK Weir are replaced with those of Labyrinth Weir (Paxson, Tullis and Hertel, 2014)

However, that cost difference decreases to 10% with PK Weir having cheaper construction cost than Labyrinth Weir when channel application has fixed spillway channel length and requires a concrete lining (slab) and training walls, as seen in Figure 21.

2.4.5 Literature on the physical modelling and Froude number

Physical hydraulic model is a smaller-size, laboratory-scaled representation of a full-scale hydraulic structure. Hydraulic structures could be dams, weirs, flumes, water wheels, etc. Similarities in form (geometric), motion (kinematic) and forces (dynamic) between laboratory models and full scape prototypes are critically required (Chanson, 1999).

Physical modelling is used during design phases to optimize and ensure safety in operations of the structure. It is also helpful in experiencing and visualizing the structure before constructing and operating in real life (Chanson, 1999).

The Froude number, naming after the French researcher William Froude, is a dimensionless number used typically for free surface flows, hydraulic structures such as weirs and open spillways scaling methods (Chanson, 1999).

$$\mathbf{Fr} = \frac{\mathbf{V}}{\sqrt{\mathbf{g} \times \mathbf{L}}}$$

where V is velocity, g is acceleration of gravity and L is length

A scale ratio should be determined for each circumstance where Froude number of full-scale prototypes (p) is proportional to laboratory-scale models (m) $Fr_p = Fr_m$. Other derived scale ratios (r = p/m) are:

1. Velocity $\mathbf{V_r} = \sqrt{\mathbf{L_r}}$
2. Discharge $\mathbf{Q_r} = \mathbf{V_r} \times \mathbf{L_r}^{\mathbf{2}} = \mathbf{L_r}^{\frac{\mathbf{5}}{\mathbf{2}}}$
3. Force $\mathbf{F_r} = \frac{\mathbf{Mr} \times \mathbf{Lr}}{\mathbf{Tr}^{\mathbf{2}}} = \mathbf{p} \times \mathbf{L_r}^{\mathbf{3}}$
4. Pressure $\mathbf{P_r} = \frac{\mathbf{Fr}}{\mathbf{Lr}^{\mathbf{2}}} = \mathbf{p_r} \times \mathbf{L_r}$

Table 1. Summary of Literature Search

Citation	Type	Significant Outcome
Anderson, 2011	Thesis	Gives insights about the similar experiments on Piano Key Weirs and Trapezoidal Labyrinth Weirs.
Businge, 2020	Thesis	Gives guidelines and recommendations about the similar study. Provides results and analyses for the experiments on a Trapezoidal Labyrinth Weir.
Barcouda et al., 2006	Conference prodceedings	Explains the effects of crest shape on PK Weir's discharge efficiency.
Chanson, 1999	Book	Explains the physical modelling of hydraulics.
Engineering Notes, 2020	Article	Classifies types of notches and weirs.
Hillhouse, 2019	Article	Explains the definition of weirs.
Hanania et al., 2017	Article	Explains the definition of weirs.
Idrees, Al-Ameri and Das, (2016)	Article	Explains the impact of Labyrinth Weir orientations on the discharge efficiency.
Lemperiere and Ouamane, 2003	Article	Explains PK Weir.
Machiels, Erpicum, Archambeau, Dewals and Pirotton, 2012	Article	Explains different types of PK Weirs and their discharge efficiency.
Open Channel Flow, 2020	Article	Explains aerations of weir nappes.
Ouamane and Lemperiere, 2006	Article	Explains the effects of fillets on PK Weir.
Peter, 1994	Article	Recommends the discharge coefficients for different crest shapes.
Paxson, Tullis and Hertel, 2014	Article	Compare PK Weir with Labyrinth Weir in terms of hydraulics, cost, constructability, and operations.

Ribeiro et al., 2009	Article	Explains different types of PK Weirs and their discharge efficiencies.
Ribeiro, Boillat, Schleiss, Laugier and Albalat, 2007	Article	Explains the effects of crest shape on PK Weir's discharge efficiency.
Riberio et al., 2007	Article	Explains the effects of crest shape on PK Weir's discharge efficiency.
Schleiss, 2011	Article	Explains different types of PK Weirs.
Truong, Ho and Dinh, 2006	Article	Explains different nappe behaviors of PK Weir.
Young, 2018	Thesis	Explains different nappe behaviors of PK Weir.

2.5 **Summary of Chapter**

This chapter has presented the overview of the extant literature, its place of publication, the methodology used, the differences between the literature and the proposed research, the weaknesses in the found literature that have been strengthened in this research and the results of the found literature.

Topics such as different type of PK Weirs, vented versus unvented overflow, effect of weir orientation on Labyrinth Weirs and cost comparison between PK Weir and Labyrinth Weir have been discussed.

3 METHODOLOGY

This chapter describes the methods adopted from the extant research in the literature review chapter. The methodology adopted here is a laboratory experiment that is done with the same aim as the found research, which is to predict the discharge coefficient of a PK Weir and compare it with a Labyrinth Weir.

3.1 Experimental setup

Laboratory experiments in this research were carried out in a rectangular flume in the Hydraulic Laboratory of Mainz University of Applied Sciences, Germany.

Figure 22. The hydraulic equipment of Mainz University of Applied Sciences' Hydraulic Laboratory for this research (HS Mainz, 2020)

In this research, laboratory models of a PK Weir and a Labyrinth Weir were examined in a rectangular flume with the dimensions of 10 m long, 0.30 m wide and 0.47 m deep. Transparent glass flume side walls allowed visual observations such as water surface profile and flow conditions (HS Mainz, 2020). The flume and flume equipment used in this research are shown below in Figures 22 and 23.

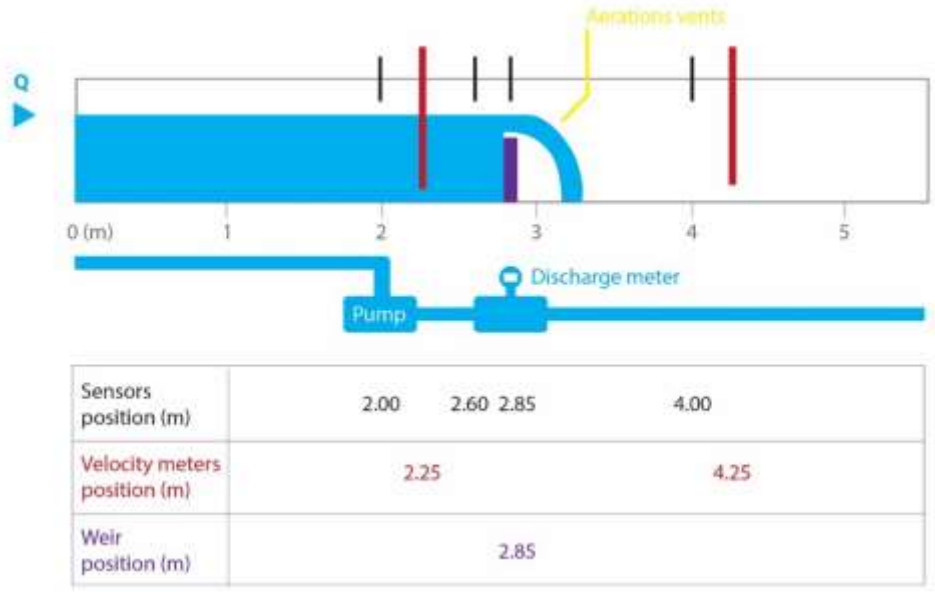

Figure 23. Scheme of the Testing Flume setup

The water supply for Mainz University of Applied Sciences Hydraulic Lab is provided by City of Mainz. The water is fed and cycled throughout the flume using a pump with the maximum capacity of 21 l/s.

Measuring devices used in this research were an Ultrasonic Sensor Device UltraLab ULS HF54/58 with multiple sensors, a Propeller Flow Meter, and a Magnetic Flow Meter (HS Mainz, 2020). According to General Acoustics (2017), “UltraLab ULS HF54/58 is a Sophisticated Level and Wave Measurement for Labs.”. It is a high speed, calibration-free measurement system based on General Acoustics’ innovative ultrasound technology.

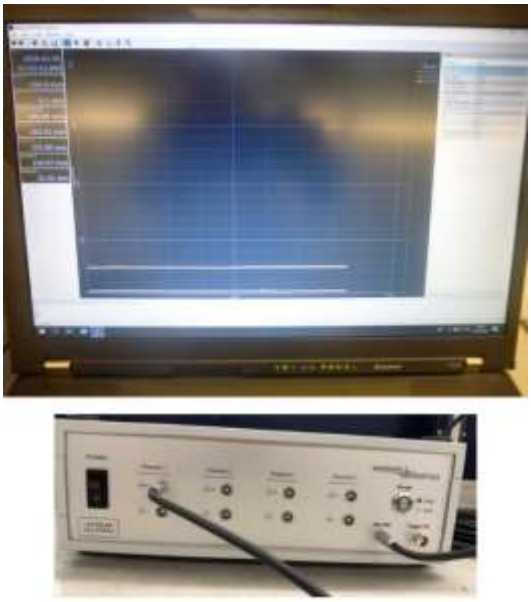

Figure 24. UltraLab ULS HF54/58 setup with the monitor to record the readings (HS Mainz, 2020)

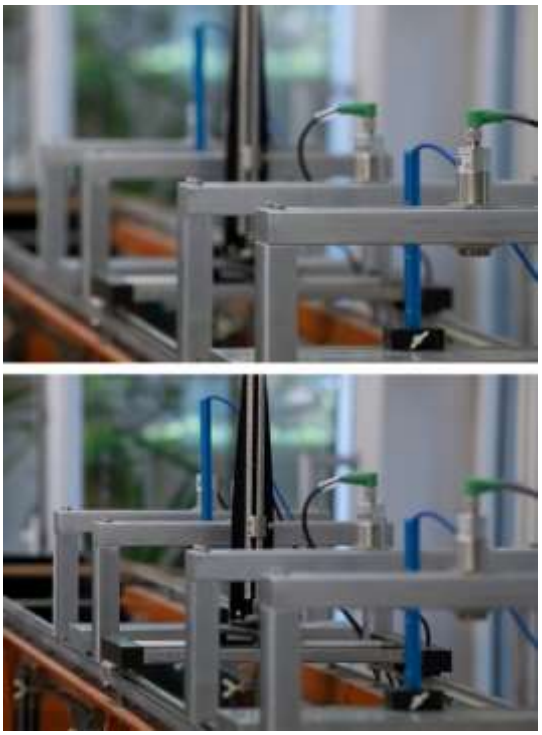

Figure 25. The sensors located along the flume to measure the water level. There are 4 ultrasonic sensors and 2 velocity meters, in blue
(HS Mainz, 2020)

Propeller Flow Meter is a fluid velocity measuring device using a propeller. Fluid's mechanical energy is used in rotating the pinwheel (rotor) while blades on the rotor are angled to transform energy from the stream into rotational energy. The rotor spins proportionally faster when the fluid moves faster accordingly (Universal Flow Monitors, 2020).

Figure 26. Propeller Flow Meter used to measure the fluid velocity
(HS Mainz, 2020)

Magnetic Flow Meter measures the flow of the fluid in a pipe by using Faraday's Law of Electromagnetic Induction (Universal Flow Monitors, 2020). In this experiment, the Meter enabled to set the water flow in the flume at required discharges.

Figure 27. Set up of Magnetic Flow Meter and Propeller Flow Meter
(HS Mainz, 2020)

Models of weirs were made of acrylic sheets and were cut out by CNC machine according to the design specifications. The weirs were assembled with glue. Weirs were attached to the base using gum.

Figure 28. Model of the PK Weir used in the research, with ramps in the outlet cycle (HS Mainz, 2020)

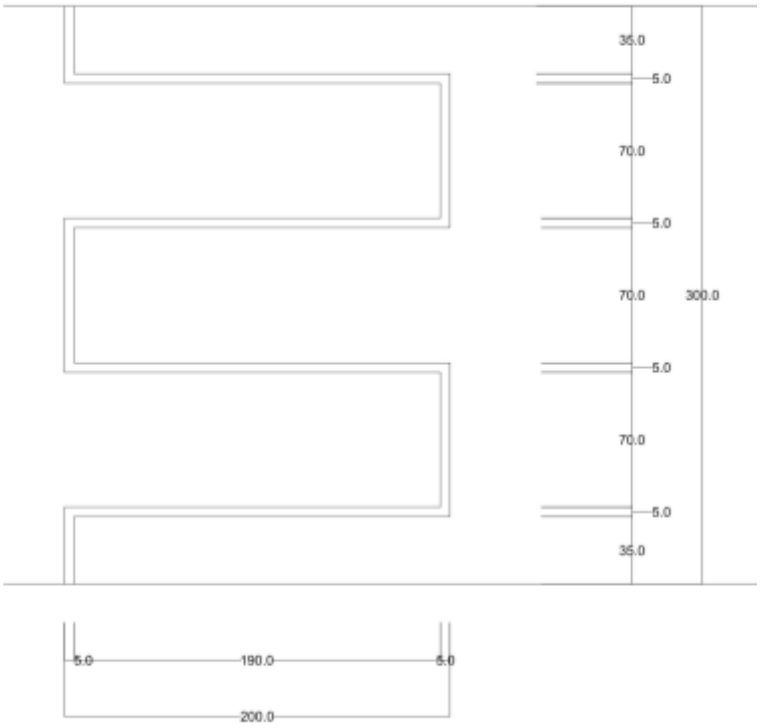

Figure 29. Explanation of the geometries in the PK Weir, without ramps

PK Weir dimensions (HS Mainz, 2020):

- Number of cycles **N** = 2
- Total weir height **P** = 200 mm, including the base 20 mm
- Length of control footprint structure **B** = 200 mm
- Total width of the weir **W** = 300 mm
- Effective length of the weir **L** = 1100 mm

- Wall thickness **t** = 5 mm
- Angle of the weir α = 0

Figure 30. Model of the Trapezoidal Labyrinth Weir used in the research (HS Mainz, 2020)

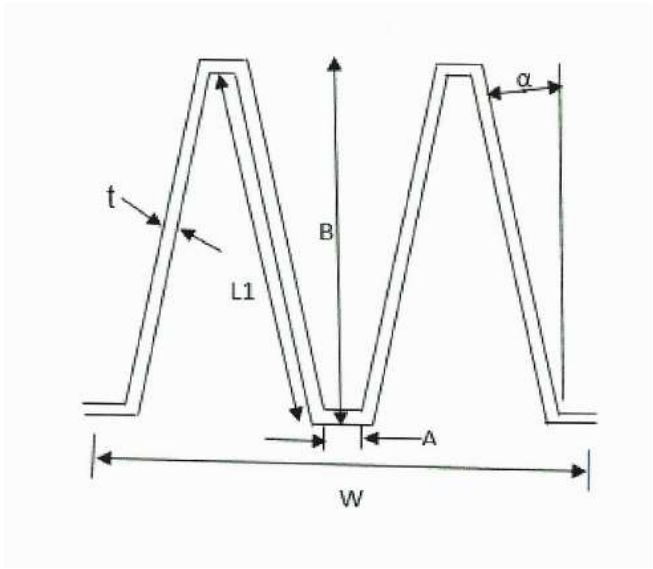

Figure 31. Explanation of the geometries in the Trapezoidal Labyrinth Weir (Businge, 2020)

Trapezoidal Labyrinth Weir dimensions (HS Mainz, 2020):

- Number of cycles **N** = 2
- Weir height **P** = 184 mm
- Length of control footprint structure **B** = 156 mm
- Total width of the weir **W** = 300 mm

- Length along crest of one arm of the weir **L1** = 158.7 mm
- Effective length of the weir **L** = 2*N*(A+L1) = 714.8 mm. (Coleman and Lindell, 2004)
- Width of interior apex **A** = 20 mm
- Wall thickness **t** = 6 mm
- Angle of the weir α = 19.1

Figure 32. Overview of PK Weir setup in the flume (HS Mainz, 2020)

Figure 33. Overview of Labyrinth Weir setup in the flume
(HS Mainz, 2020)

3.2 **Experimental procedure**

The experimental procedure is as follows (HS Mainz, 2020):

1. Fit the weir to the weir carrier which is bonded in the channel and tighten it with a thumb nut below to make it firm enough inside the flume.
2. Gum is placed on the sides and underneath the weir to allow water flowing only over the weir crest.
3. Place the UltraLab ULS HF54/58 sensors and Propeller Flow Meters in their respective positions and make necessary adjustments with the help from the measuring software to make accurate measurements for the water level.
4. Start the pump, increase the discharge till water is circulated in the flume and starts to flow over the weir. The discharge is re-adjusted to the required flow for measurement.
5. (For the vented cases only) Place the nappe venting devices. These should be placed above the maximum water level of the weir to ensure the nappe stays aerated for all flows.
6. For each discharge ranging from 1 l/s to 21 l/s, the corresponding water levels and velocities, both upstream and downstream were recorded to the UltraLab software.
7. Replace the PK Weir with the Labyrinth Weir and repeat the same procedure.
8. All data were collected from the UltraLab software's sheets in order to make calculations for the Discharge Coefficients and Head over Height of Weir ratios.

3.3 **Number of Experiments**

From the Poleni equation (1a), it can be transformed below to calculate the Discharge Coefficient of both PK Weir and Trapezoidal Labyrinth Weir:

$$C_d = \frac{Q}{\frac{2}{3} \times L \times \sqrt{2g} \times {H_t}^{\frac{3}{2}}} \tag{3}$$

Adding the dimensions from the scaled models of PK Weir and TL Weir, we have the C_d equation used for PK Weir and TL Weir, in equation (3a) and (3b) respectively below:

substituting L = 1100 mm, g = 9.81 m/s^2 give $C_d = \frac{Q}{3.25 \times {H_t}^{\frac{3}{2}}}$ (3a)

substituting L = 714.8 mm, g = 9.81 m/s^2 give $C_d = \frac{Q}{2.11 \times H_t^{\frac{3}{2}}}$ (3b)

where C_d is discharge coefficient
Q is discharge
L (mm) is total effective length of weir
g (m/s^2) is gravitational constant = 9.81
H_t (mm) is the total head

Table 2 below shows the testing matrix for this experiment. In this research, Piano Key Weir (PK) terms are comparable with Rectangular Labyrinth Weir (RL) in Anderson (2011).

Table 2. Testing Matrix

	Experiment	Abbreviation
1	Flow over a PK Weir without ramps and without aeration vents (U = Unvented)	PK-U
2	Flow over a PK Weir with ramps in the outlet, without aeration vents	PKRO-U
3	Flow over a PK Weir with ramps in the inlet, without aeration vents	PKRI-U
4	Flow over a Trapezoidal Labyrinth Weir, normal orientation (M-shape) without aeration vents	TLM-U
5	Flow over a Trapezoidal Labyrinth Weir, inverse orientation (W-shape) without aeration vents	TLW-U
6	Flow over a PK Weir without ramps, with aeration vents (V = Vented)	PK-V
7	Flow over a PK Weir with ramps in the outlet and with aeration vents	PKRO-V
8	Flow over a PK Weir with ramps in the inlet and with aeration vents	PKRI-V
9	Flow over a Trapezoidal Labyrinth Weir, normal orientation (M-shape) with aeration vents	TLM-V
10	Flow over a Trapezoidal Labyrinth Weir, inverse orientation (W-shape) with aeration vents	TLW-V

3.4 **Summary of Chapter**

This chapter has described the methodology adopted from the found literature and explained the reasons why it was adopted, and included a description of the experimental setup and the experimental procedure.

4 **DATA PRESENTATION AND ANALYSIS**

This chapter presents the results from the hypothetical data of the PK Weir and the results from the previous experiments conducted in the laboratory for this research.

In Chapter 2.4.5, the discharge scaling ratio $\mathbf{Q_r = L_r^{\frac{5}{2}}}$ was presented, with r being the ratio between the full-scale model and the smaller scale model. In Figure 12, there is a difference in Trapezoidal Labyrinth Weir (TL) and Rectangular Labyrinth Weir (RL) curves (Anderson, 2011). The discharge coefficient of TL is higher than that of RL. Based on that, the scaling ratio is drawn using the weir heights (P, in mm) of TL and RL from Anderson's research (2011).

$$\frac{\mathbf{Q_{TL,\,Anderson}}}{\mathbf{Q_{RL,\,Anderson}}} = \left(\frac{\mathbf{P_{TL,\,Anderson}}}{\mathbf{P_{RL,\,Anderson}}}\right)^{\mathbf{2.5}}$$

Then

$$\mathbf{Q_{TL,\,Anderson}} = \left(\frac{\mathbf{P_{TL,\,Anderson}}}{\mathbf{P_{RL,\,Anderson}}}\right)^{\mathbf{2.5}} \times \mathbf{Q_{RL,\,Anderson}} = \mathbf{x^{2.5}} \times \mathbf{Q_{RL,\,Anderson}}$$

where **x** is the scaling ratio. Replacing $\mathbf{P_{TL,\,Anderson}}$ = 8.75" = 222.25 mm and $\mathbf{P_{RL,\,Anderson}}$ = 7.75'' = 196.85 mm (Anderson, 2011) gives **x** = 1.357.

One scale ratio derived from Froude number (Chanson, 1999) is the water depth:

$$\mathbf{H_{t,\,TL,\,Anderson} = x * H_{t,\,RL,\,Anderson}}$$

Likewise, the scaling ratio method was adapted to this research as follows:

1. The discharges of PK-U and PK-V were predicted by adapting from the discharge of TLW-U, TLM-U, TLW-V and TLM-V (Businge, 2020) since the flume and the pump capacity were similar.
2. The water depth of PK-U and PK-V were predicted by calculating from the water depth of TLW-U, TLM-U, TLW-V and TLM-V (Businge, 2020) using formula $\mathbf{H_{t,\,PK,\,Vinh}} = \frac{\mathbf{H_{t,\,TL,\,Businge}}}{x}$.
3. The discharge coefficients were predicted by calculating from the equation (3a) above.
4. Lastly, the predicted results of PKRO and PKRI (vented and unvented) were calculated using the same method, with the addition of 1% and 2% respectively.

4.1 **Tables of Predicted Results for PK Weir (The Author, 2020)**

Table 3. Results of Unvented PK Weir, without ramps (PK-U)

Run	Q (l/s)	Q (m3/s)	Ht (mm)	Ht (m)	Calculated Cd	Ht/P
1	1.02	0.0010	8.85	0.0089	0.3761	0.0443
2	2.02	0.0020	13.28	0.0133	0.4055	0.0664
3	3.00	0.0030	15.93	0.0159	0.4581	0.0797
4	4.02	0.0040	19.47	0.0195	0.4543	0.0974
5	5.00	0.0050	21.24	0.0212	0.4959	0.1062
6	6.03	0.0060	24.78	0.0248	0.4746	0.1239
7	7.02	0.0070	30.98	0.0310	0.3953	0.1549
8	8.01	0.0080	34.52	0.0345	0.3835	0.1726
9	9.06	0.0091	38.06	0.0381	0.3747	0.1903
10	10.06	0.0101	41.60	0.0416	0.3641	0.2080
11	11.00	0.0110	45.14	0.0451	0.3522	0.2257
12	12.00	0.0120	47.79	0.0478	0.3526	0.2390
13	13.02	0.0130	51.33	0.0513	0.3437	0.2567
14	14.01	0.0140	53.99	0.0540	0.3429	0.2699
15	15.00	0.0150	57.53	0.0575	0.3338	0.2876
16	16.03	0.0160	60.18	0.0602	0.3333	0.3009
17	17.04	0.0170	62.84	0.0628	0.3321	0.3142
18	18.00	0.0180	65.49	0.0655	0.3297	0.3275
19	19.02	0.0190	68.15	0.0681	0.3282	0.3407
20	20.00	0.0200	70.80	0.0708	0.3259	0.3540
21	21.00	0.0210	72.57	0.0726	0.3298	0.3629

Table 4. Results of Unvented PK Weir, with outlet ramps (PKRO-U)

Run	Q (l/s)	Q (m3/s)	Ht (mm)	Ht (m)	Calculated Cd	Ht/P
1	1.02	0.0010	8.94	0.0089	0.3705	0.0447
2	2.02	0.0020	13.41	0.0134	0.3994	0.0670
3	3.00	0.0030	16.09	0.0161	0.4513	0.0804
4	4.02	0.0040	19.66	0.0197	0.4475	0.0983
5	5.00	0.0050	21.45	0.0215	0.4885	0.1073
6	6.03	0.0060	25.03	0.0250	0.4675	0.1251
7	7.02	0.0070	31.28	0.0313	0.3895	0.1564
8	8.01	0.0080	34.86	0.0349	0.3778	0.1743
9	9.06	0.0091	38.44	0.0384	0.3691	0.1922
10	10.06	0.0101	42.01	0.0420	0.3587	0.2101
11	11.00	0.0110	45.59	0.0456	0.3470	0.2279
12	12.00	0.0120	48.27	0.0483	0.3474	0.2413
13	13.02	0.0130	51.84	0.0518	0.3386	0.2592
14	14.01	0.0140	54.52	0.0545	0.3378	0.2726
15	15.00	0.0150	58.10	0.0581	0.3288	0.2905
16	16.03	0.0160	60.78	0.0608	0.3284	0.3039
17	17.04	0.0170	63.46	0.0635	0.3272	0.3173
18	18.00	0.0180	66.14	0.0661	0.3248	0.3307
19	19.02	0.0190	68.83	0.0688	0.3234	0.3441
20	20.00	0.0200	71.51	0.0715	0.3211	0.3575
21	21.00	0.0210	73.30	0.0733	0.3249	0.3665

Table 5. Results of Unvented PK Weir, with inlet ramps (PKRI-U)

Run	Q (l/s)	Q (m3/s)	Ht (mm)	Ht (m)	Calculated Cd	Ht/P
1	1.02	0.0010	9.03	0.0090	0.3651	0.0451
2	2.02	0.0020	13.54	0.0135	0.3936	0.0677
3	3.00	0.0030	16.25	0.0162	0.4447	0.0812
4	4.02	0.0040	19.86	0.0199	0.4410	0.0993
5	5.00	0.0050	21.66	0.0217	0.4814	0.1083
6	6.03	0.0060	25.28	0.0253	0.4607	0.1264
7	7.02	0.0070	31.59	0.0316	0.3838	0.1580
8	8.01	0.0080	35.21	0.0352	0.3723	0.1760
9	9.06	0.0091	38.82	0.0388	0.3637	0.1941
10	10.06	0.0101	42.43	0.0424	0.3534	0.2121
11	11.00	0.0110	46.04	0.0460	0.3419	0.2302
12	12.00	0.0120	48.75	0.0487	0.3423	0.2437
13	13.02	0.0130	52.36	0.0524	0.3337	0.2618
14	14.01	0.0140	55.06	0.0551	0.3329	0.2753
15	15.00	0.0150	58.68	0.0587	0.3240	0.2934
16	16.03	0.0160	61.38	0.0614	0.3236	0.3069
17	17.04	0.0170	64.09	0.0641	0.3224	0.3205
18	18.00	0.0180	66.80	0.0668	0.3201	0.3340
19	19.02	0.0190	69.51	0.0695	0.3186	0.3475
20	20.00	0.0200	72.22	0.0722	0.3164	0.3611
21	21.00	0.0210	74.02	0.0740	0.3201	0.3701

Table 6. Results of Vented PK Weir, without ramps (PK-V)

Run	Q (l/s)	Q (m3/s)	Ht (mm)	Ht (m)	Calculated Cd	Ht/P
1	1.00	0.0010	8.85	0.0089	0.3687	0.0443
2	2.00	0.0020	13.28	0.0133	0.4014	0.0664
3	3.00	0.0030	16.82	0.0168	0.4224	0.0841
4	4.03	0.0040	20.36	0.0204	0.4260	0.1018
5	5.05	0.0051	24.78	0.0248	0.3974	0.1239
6	6.00	0.0060	27.44	0.0274	0.4054	0.1372
7	7.00	0.0070	31.86	0.0319	0.3779	0.1593
8	8.00	0.0080	35.40	0.0354	0.3687	0.1770
9	9.05	0.0091	38.94	0.0389	0.3616	0.1947
10	10.01	0.0100	42.48	0.0425	0.3510	0.2124
11	11.00	0.0110	46.02	0.0460	0.3421	0.2301
12	12.00	0.0120	48.68	0.0487	0.3431	0.2434
13	13.05	0.0131	53.10	0.0531	0.3274	0.2655
14	14.01	0.0140	55.76	0.0558	0.3267	0.2788
15	15.05	0.0151	59.30	0.0593	0.3200	0.2965
16	16.05	0.0161	62.84	0.0628	0.3128	0.3142
17	17.02	0.0170	66.38	0.0664	0.3056	0.3319
18	18.00	0.0180	69.03	0.0690	0.3047	0.3452
19	19.03	0.0190	72.57	0.0726	0.2988	0.3629
20	20.04	0.0200	76.11	0.0761	0.2930	0.3806
21	21.00	0.0210	78.77	0.0788	0.2916	0.3938

Table 7. Results of Vented PK Weir, with outlet ramps (PKRO-V)

Run	Q (l/s)	Q (m3/s)	Ht (mm)	Ht (m)	Calculated Cd	Ht/P
1	1.00	0.0010	8.94	0.0089	0.3633	0.0447
2	2.00	0.0020	13.41	0.0134	0.3955	0.0670
3	3.00	0.0030	16.98	0.0170	0.4161	0.0849
4	4.03	0.0040	20.56	0.0206	0.4197	0.1028
5	5.05	0.0051	25.03	0.0250	0.3916	0.1251
6	6.00	0.0060	27.71	0.0277	0.3993	0.1385
7	7.00	0.0070	32.18	0.0322	0.3723	0.1609
8	8.00	0.0080	35.75	0.0358	0.3633	0.1788
9	9.05	0.0091	39.33	0.0393	0.3562	0.1966
10	10.01	0.0100	42.90	0.0429	0.3458	0.2145
11	11.00	0.0110	46.48	0.0465	0.3370	0.2324
12	12.00	0.0120	49.16	0.0492	0.3380	0.2458
13	13.05	0.0131	53.63	0.0536	0.3226	0.2682
14	14.01	0.0140	56.31	0.0563	0.3219	0.2816
15	15.05	0.0151	59.89	0.0599	0.3153	0.2994
16	16.05	0.0161	63.46	0.0635	0.3082	0.3173
17	17.02	0.0170	67.04	0.0670	0.3010	0.3352
18	18.00	0.0180	69.72	0.0697	0.3002	0.3486
19	19.03	0.0190	73.30	0.0733	0.2944	0.3665
20	20.04	0.0200	76.87	0.0769	0.2887	0.3844
21	21.00	0.0210	79.55	0.0796	0.2873	0.3978

Table 8. Results of Vented PK Weir, with inlet ramps (PKRI-V)

Run	Q (l/s)	Q (m3/s)	Ht (mm)	Ht (m)	Calculated Cd	Ht/P
1	1.00	0.0010	9.03	0.0090	0.3580	0.0451
2	2.00	0.0020	13.54	0.0135	0.3897	0.0677
3	3.00	0.0030	17.15	0.0172	0.4100	0.0858
4	4.03	0.0040	20.76	0.0208	0.4136	0.1038
5	5.05	0.0051	25.28	0.0253	0.3858	0.1264
6	6.00	0.0060	27.98	0.0280	0.3935	0.1399
7	7.00	0.0070	32.50	0.0325	0.3668	0.1625
8	8.00	0.0080	36.11	0.0361	0.3580	0.1805
9	9.05	0.0091	39.72	0.0397	0.3510	0.1986
10	10.01	0.0100	43.33	0.0433	0.3407	0.2166
11	11.00	0.0110	46.94	0.0469	0.3321	0.2347
12	12.00	0.0120	49.65	0.0496	0.3330	0.2482
13	13.05	0.0131	54.16	0.0542	0.3178	0.2708
14	14.01	0.0140	56.87	0.0569	0.3171	0.2844
15	15.05	0.0151	60.48	0.0605	0.3106	0.3024
16	16.05	0.0161	64.09	0.0641	0.3037	0.3205
17	17.02	0.0170	67.70	0.0677	0.2966	0.3385
18	18.00	0.0180	70.41	0.0704	0.2958	0.3521
19	19.03	0.0190	74.02	0.0740	0.2901	0.3701
20	20.04	0.0200	77.63	0.0776	0.2844	0.3882
21	21.00	0.0210	80.34	0.0803	0.2831	0.4017

4.2 Tables of Results for Trapezoidal Labyrinth Weir (Businge, 2020)

Table 9. Results of Unvented Trapezoidal Labyrinth Weirs (TLM-U and TLW-U). Both had the same results (Businge, 2020)

Run	Q (l/s)	Q (m3/s)	Ht (mm)	Ht (m)	Calculated Cd	Ht/P
1	1.02	0.0010	10	0.0100	0.4835	0.0543
2	2.02	0.0020	15	0.0150	0.5212	0.0815
3	3.00	0.0030	18	0.0180	0.5888	0.0978
4	4.02	0.0040	22	0.0220	0.5839	0.1196
5	5.00	0.0050	24	0.0240	0.6374	0.1304
6	6.03	0.0060	28	0.0280	0.6100	0.1522
7	7.02	0.0070	35	0.0350	0.5082	0.1902
8	8.01	0.0080	39	0.0390	0.4930	0.2120
9	9.06	0.0091	43	0.0430	0.4816	0.2337
10	10.06	0.0101	47	0.0470	0.4680	0.2554
11	11.00	0.0110	51	0.0510	0.4527	0.2772
12	12.00	0.0120	54	0.0540	0.4533	0.2935
13	13.02	0.0130	58	0.0580	0.4418	0.3152
14	14.01	0.0140	61	0.0610	0.4408	0.3315
15	15.00	0.0150	65	0.0650	0.4290	0.3533
16	16.03	0.0160	68	0.0680	0.4285	0.3696
17	17.04	0.0170	71	0.0710	0.4269	0.3859
18	18.00	0.0180	74	0.0740	0.4238	0.4022
19	19.02	0.0190	77	0.0770	0.4219	0.4185
20	20.00	0.0200	80	0.0800	0.4190	0.4348
21	21.00	0.0210	82	0.0820	0.4239	0.4457

Table 10. Results of Vented Trapezoidal Labyrinth Weirs, normal orientation (TLM-V) (Businge, 2020)

Run	Q (l/s)	Q (m3/s)	Ht (mm)	Ht (m)	Calculated Cd	Ht/P
1	1.00	0.0010	10	0.010	0.4740	0.0543
2	2.00	0.0020	15	0.015	0.5160	0.0815
3	3.00	0.0030	19	0.019	0.5430	0.1033
4	4.03	0.0040	23	0.023	0.5476	0.1250
5	5.05	0.0051	28	0.028	0.5109	0.1522
6	6.00	0.0060	31	0.031	0.5211	0.1685
7	7.00	0.0070	36	0.036	0.4858	0.1957
8	8.00	0.0080	40	0.040	0.4740	0.2174
9	9.05	0.0091	44	0.044	0.4648	0.2391
10	10.01	0.0100	48	0.048	0.4512	0.2609
11	11.00	0.0110	52	0.052	0.4397	0.2826
12	12.00	0.0120	55	0.055	0.4410	0.2989
13	13.05	0.0131	60	0.060	0.4209	0.3261
14	14.01	0.0140	63	0.063	0.4200	0.3424
15	15.05	0.0151	67	0.067	0.4113	0.3641
16	16.05	0.0161	71	0.071	0.4021	0.3859
17	17.02	0.0170	75	0.075	0.3928	0.4076
18	18.00	0.0180	78	0.078	0.3917	0.4239
19	19.03	0.0190	82	0.082	0.3841	0.4457
20	20.04	0.0200	86	0.086	0.3766	0.4674
21	21.00	0.0210	89	0.089	0.3749	0.4837

Table 11. Results of Vented Trapezoidal Labyrinth Weirs, inverse orientation (TLW-V) (Businge, 2020)

Run	Q (l/s)	Q (m3/s)	Ht (mm)	Ht (m)	Calculated Cd	Ht/P
1	1.00	0.0010	10	0.0100	0.4740	0.0543
2	2.07	0.0021	15	0.0150	0.5341	0.0815
3	3.06	0.0031	19	0.0190	0.5538	0.1033
4	4.01	0.0040	23	0.0230	0.5449	0.1250
5	5.03	0.0050	28	0.0280	0.5089	0.1522
6	6.05	0.0061	32	0.0320	0.5010	0.1739
7	7.05	0.0071	36	0.0360	0.4892	0.1957
8	8.02	0.0080	40	0.0400	0.4752	0.2174
9	9.05	0.0091	44	0.0440	0.4648	0.2391
10	10.00	0.0100	48	0.0480	0.4507	0.2609
11	11.05	0.0111	52	0.0520	0.4417	0.2826
12	12.06	0.0121	56	0.0560	0.4314	0.3043
13	13.04	0.0130	60	0.0600	0.4206	0.3261
14	14.05	0.0141	64	0.0640	0.4113	0.3478
15	15.00	0.0150	67	0.0670	0.4100	0.3641
16	16.00	0.0160	71	0.0710	0.4009	0.3859
17	17.02	0.0170	74	0.0740	0.4008	0.4022
18	18.01	0.0180	78	0.0780	0.3919	0.4239
19	19.00	0.0190	82	0.0820	0.3835	0.4457
20	20.03	0.0200	85	0.0850	0.3831	0.4620
21	21.00	0.0210	88	0.0880	0.3813	0.4783

4.3 **Summary of Chapter**

This chapter has presented Tables of Predicted Results for PK Weir (The Author, 2020) and Table of Results for Trapezoidal Labyrinth Weir (Businge, 2020). Results and analysis will be discussed in the next chapter.

5 DISCUSSIONS AND RECOMMENDATIONS

This chapter discusses the results and reviews the methodology used.

5.1 Discussion of Results

This research project was undertaken with the aim of Predicting the Discharge Coefficient of a scaled model Piano Key Weir from hypothetical data and comparing it with a Trapezoidal Labyrinth Weir.

$$C_d = \frac{Q}{\frac{2}{3}\times L\times\sqrt{2g}\times H_t^{\frac{3}{2}}} \quad (3a)$$

In the equation (3a) above, the discharge efficiency of a weir is not only a function of the discharge per unit weir length (C_d) but also the amount of weir length that will fit within a given restricted footprint (i.e., fixed width of weir W and/or footprint length B). Moreover, if more L can fit within the given fixed W and B, an increase in discharge efficiency at a given value of H_t may be recognized even if the C_d values are lower for that particular weir geometry (Anderson, 2011).

From the tables of results in Chapter 4, the following graphs will be explained:

1. A graph of discharge versus water level for both PK Weir and TL Weir in vented situation (PK-V, PKRO-V, PKRI-V, TLM-V, TLW-V).
2. A graph of discharge versus water level for both PK Weir and TL Weir in unvented situation (PK-U, PKRO-U, PKRI-U, TLM-U, TLW-U).
3. A graph of discharge coefficient versus head over weir height for the vented situation (PK-V, PKRO-V, PKRI-V, TLM-V, TLW-V).
4. A graph of discharge coefficient versus head over weir height for the unvented situation (PK-U, PKRO-U, PKRI-U, TLM-U, TLW-U).
5. A graph of discharge coefficient versus head over weir height for PK Weir (PK-U, PKRO-U, PKRI-U, PK-V, PKRO-V, PKRI-V).
6. A graph of discharge coefficient versus head over weir height for the M-shape and W-shape TL Weir (TLM-U, TLW-U, TLM-V, TLW-V).

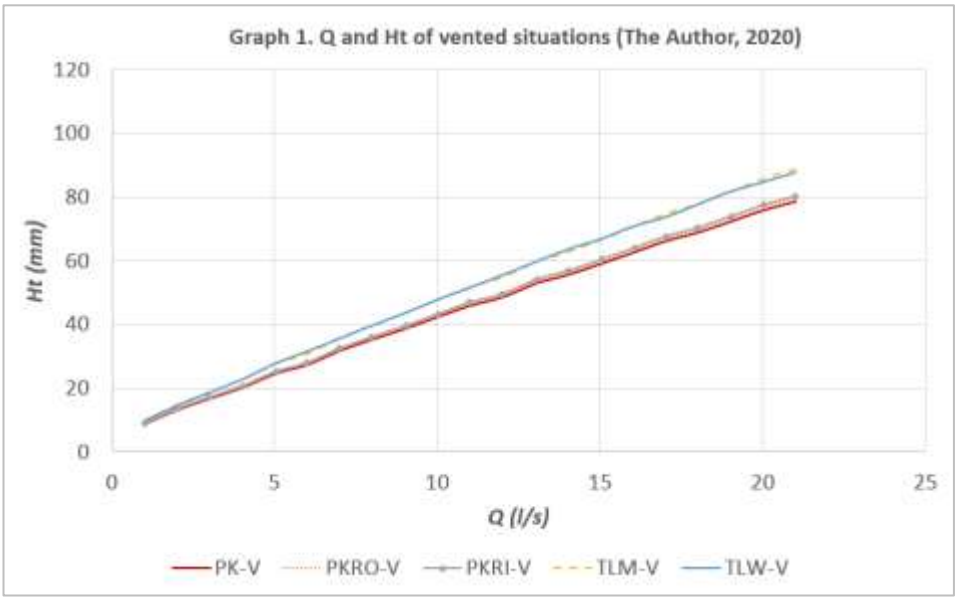

Graph 1. Discharge Q versus water level H_t of vented situations for both PK Weir and TL Weir

From Graph 1, the water levels of TL Weir and PK Weir start to differ from 1 l/s where the water level for TL Weir is 10 mm and for PK Weir is 9 mm, making a 1 mm difference. The differences start to increase as the discharges increase until the maximum reaching the maximum discharge at 21 l/s. The differences in water levels at discharges equal to 5 l/s, 10 l/s, 15 l/s and 21 l/s are 3 mm, 5.1 mm, 7.1 mm, and 9 mm, respectively.

From Graph 2 below, the water levels of TL Weir and PK Weir start to differ from 1 l/s where the water level for TL Weir is 10 mm and for PK Weir is 9 mm, making a 1 mm difference. The differences start to increase as the discharges increase until the maximum reaching the maximum discharge at 21 l/s. The differences in water levels at discharges equal to 5 l/s, 10 l/s, 15 l/s and 21 l/s are 2.5 mm, 5 mm, 7 mm, and 8.7 mm, respectively.

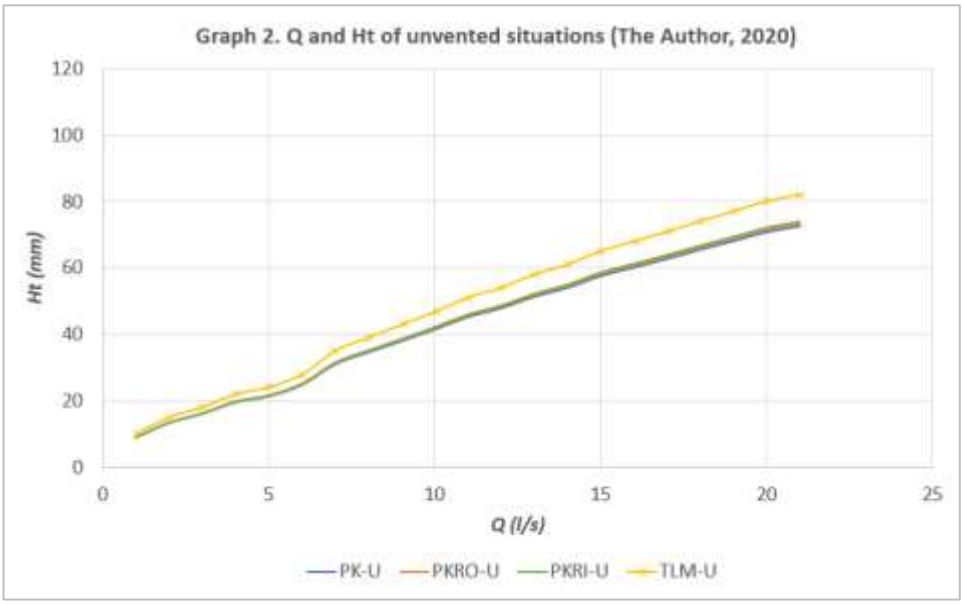

Graph 2. Discharge Q versus water level H_t of unvented situations for both PK Weir and TL Weir. TL Weir had the same results with both normal and inverse orientation

From the above observations from Graph 1 and 2, the following deductions are made:

- TL Weir experiences higher water levels than PK Weir for the same discharges, under similar flow conditions, in both vented and unvented situations.
- The differences in water levels varies between the weirs, in both vented and unvented situations. However, in general, the differences in water levels between TL Weir and PK Weir in vented situations are slightly higher.
- There are little differences between different configurations of PK Weir (with or without ramps) and TL Weir (normal and inverse orientation), both in vented and unvented situations.

The graphs below (from Graph 3 to Graph 6) provide clear understandings of the investigation on the effect of the shape of the weirs and the height of the water over the weir crest on the weir's hydraulic performances and the discharge coefficient of PK Weir and TL Weir in the same flume.

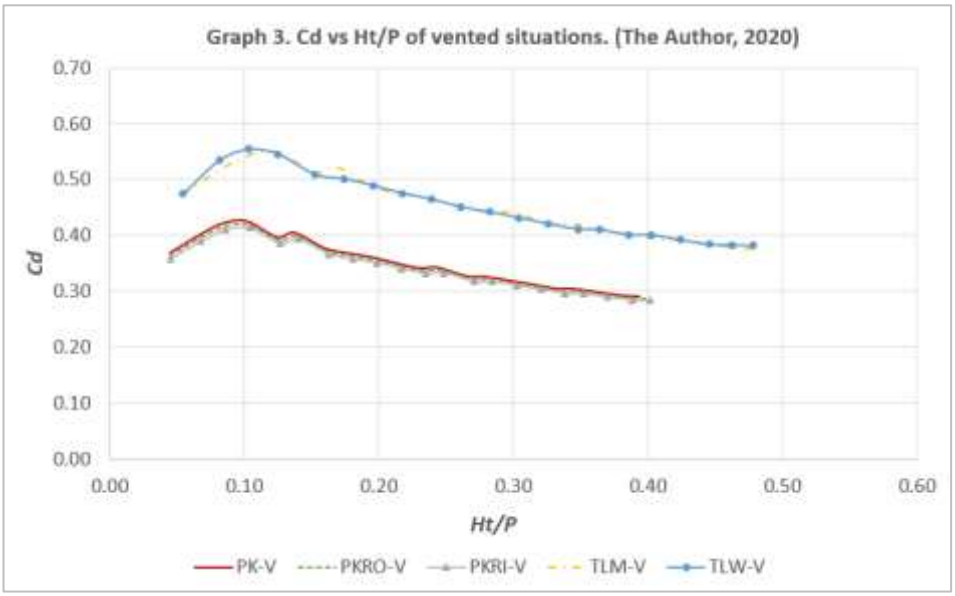

Graph 3. Discharge coefficient C_d versus head over weir height H_t/P of vented situations for both PK Weir and TL Weir

From Graph 3, TL Weir has higher discharge coefficient than PK Weir's. Both weirs have the maximum value of C_d at $H_t/P=0.1$ and have the same trend in their curves: increase from $H_t/P=0.05$ to $H_t/P=0.1$ then slightly decrease and continue to rise again and finally maintain decreasing. The differences in discharge coefficient between two weirs are maintained between 0.08 and 0.13.

The highest value of discharge coefficient of PK Weir, in vented situation, is 0.4260 at $H_t/P=0.1018$ (PK-V, without ramps) when the lowest is 0.2831 at $H_t/P=0.4017$ (PKRI-V, with inlet ramps). The highest value of discharge coefficient of TL Weir, in vented situation, is 0.5538 at $H_t/P=0.1033$ (inverse orientation) when the lowest is 0.3749 at $H_t/P=0.4837$ (normal orientation) for discharges ranging from 1 to 21 l/s.

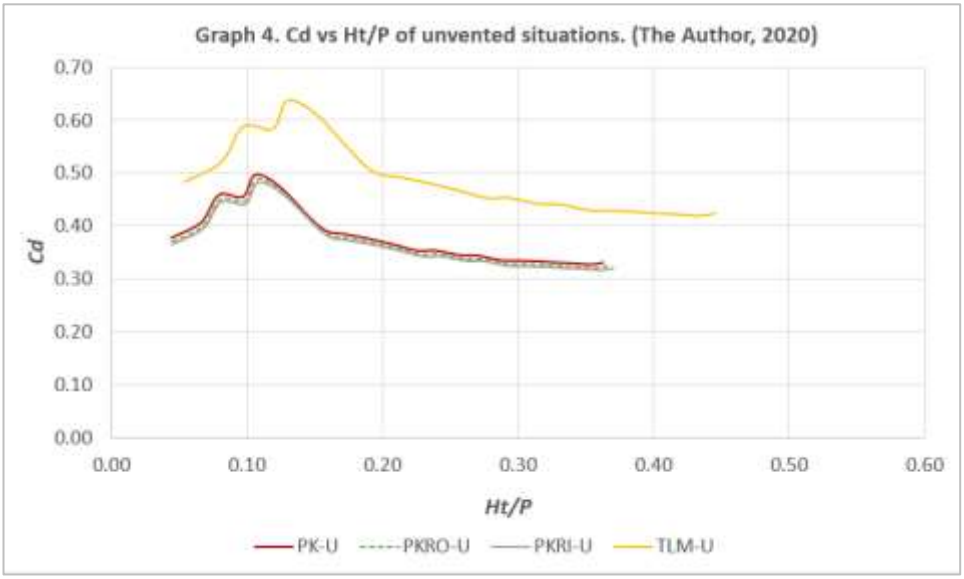

Graph 4. Discharge coefficient C_d versus head over weir height H_t/P of unvented situations for both PK Weir and TL Weir. TL Weir had the same results with both normal and inverse orientation

In Graph 4, TL Weir has higher discharge coefficient than PK Weir's with the same trend with vented situations above. The differences in discharge coefficient between two weirs are maintained between 0.09 and 0.13.

The highest value of discharge coefficient of PK Weir, in unvented situation, is 0.4959 at H_t/P=0.1062 (PK-U, without ramps) when the lowest is 0.3164 at H_t/P=0.3611 (PKRI-U, with inlet ramps). The highest value of discharge coefficient of TL Weir, in unvented situation, is 0.6374 at H_t/P=0.1304 when the lowest is 0.4190 at H_t/P=0.4348 for discharge ranging from 1 to 21 l/s.

From the Poleni equation (3a) and Graph 3 and 4, the following calculations are made to analyze the relationship between discharge coefficient and head to weir height in this experiment:

Table 12. Unvented situations PK Weir and TL Weir comparison

H_t/P	Weir	L (m)	P (m)	H_t (m)	Cd	Q (m^3/s)	Q (l/s)
0.05	PK Weir	1.100	0.200	0.010	0.4835	0.0016	1.58
	TL Weir	0.715	0.184	0.009	0.3705	0.0007	0.67
0.10	PK Weir	1.100	0.200	0.020	0.4814	0.0044	4.45
	TL Weir	0.715	0.184	0.018	0.5888	0.0030	3.02
0.13	PK Weir	1.100	0.200	0.026	0.4607	0.0063	6.31
	TL Weir	0.715	0.184	0.024	0.6374	0.0050	5.03
0.30	PK Weir	1.100	0.200	0.060	0.3284	0.0158	15.76
	TL Weir	0.715	0.184	0.055	0.4418	0.0121	12.09

In Table 12, with the same head over weir height H_t/P, unvented, PK Weir experiences higher discharge Q with lower discharge coefficient C_d, except for the ratio $H_t/P=0.05$ where PK Weir's C_d is higher than TL Weir's. The differences in discharge percentages vary:

- At $H_t/P=0.05$, PK Weir discharges 135% more than TL Weir.
- At $H_t/P=0.10$, PK Weir discharges 47% more than TL Weir.
- At $H_t/P=0.13$, PK Weir discharges 25% more than TL Weir.
- At $H_t/P=0.30$, PK Weir discharges 30% more than TL Weir.

Table 13. Vented situations PK Weir and TL Weir comparison

H_t/P	Weir	L (m)	P (m)	H_t (m)	Cd	Q (m^3/s)	Q (l/s)
0.05	PK Weir	1.100	0.200	0.010	0.3787	0.00124	1.24
	TL Weir	0.715	0.184	0.009	0.474	0.00086	0.86
0.1	PK Weir	1.100	0.200	0.020	0.4197	0.00388	3.88
	TL Weir	0.715	0.184	0.018	0.5538	0.00284	2.84
0.13	PK Weir	1.100	0.200	0.026	0.3858	0.00528	5.28
	TL Weir	0.715	0.184	0.024	0.5445	0.00430	4.30
0.3	PK Weir	1.100	0.200	0.060	0.3106	0.01490	14.90
	TL Weir	0.715	0.184	0.055	0.4314	0.01181	11.81

In Table 13, with the same head over weir height H_t/P, vented, PK Weir experiences higher discharge Q with lower discharge coefficient C_d. The differences in discharge percentages vary:

- At $H_t/P=0.05$, PK Weir discharges 44% more than TL Weir.
- At $H_t/P=0.10$, PK Weir discharges 36% more than TL Weir.
- At $H_t/P=0.13$, PK Weir discharges 23% more than TL Weir.
- At $H_t/P=0.30$, PK Weir discharges 26% more than TL Weir.

From the above observations in Graph 3 and 4, the following deductions are made:

- TL Weir has higher discharge coefficients than PK Weir, both in vented and unvented situations, under the same ratio head to weir height.
- With the same head over weir height H_t/P, in both vented and unvented situations, PK Weir experiences higher discharge Q with lower discharge coefficient C_d. PK Weir discharges, from 23% to 135% more than TL Weir.
- PK Weir has higher discharge efficiency than TL Weir with more length L can fit within the given fixed width W and breath B at a given value of H_t/P.

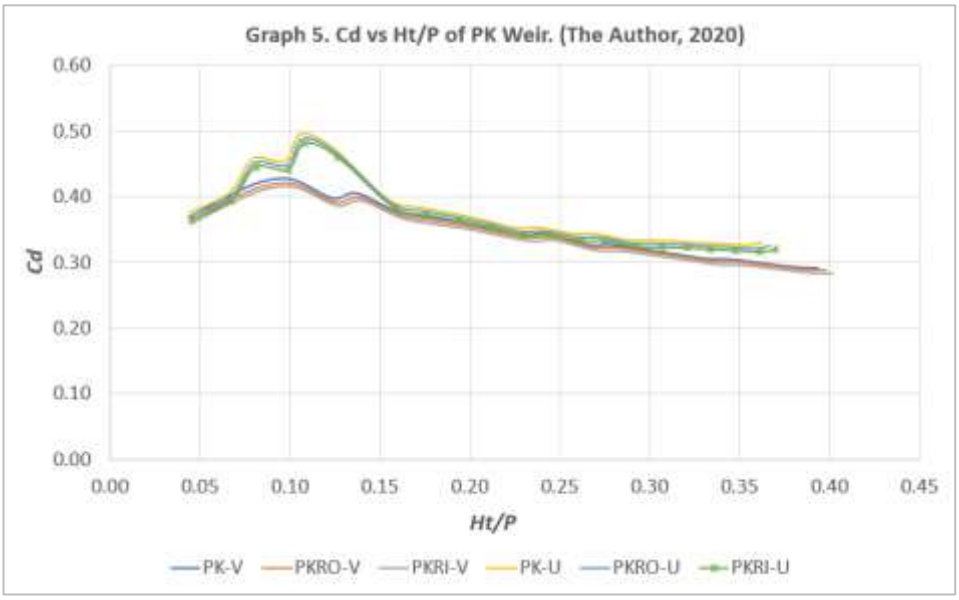

Graph 5. Discharge coefficient C_d versus head over weir height H_t/P of PK Weir, both vented and unvented situations

In Graph 5, it is seen that additional ramps have almost no effect on the discharge coefficient of PK Weir, both in vented and unvented situations. In general, PK Weir in unvented situations has slightly higher values of discharge coefficients with the same head to weir height values, compared to vented PK Weir situations.

The range of discharge coefficient of PK Weir in unvented situations are 0.3259-0.4959 for PK-U, 0.3211-0.4885 for PKRO-U and 0.3164-0.4814 for PKRI-U. The range of discharge coefficient of PK Weir in vented situations are lower, 0.2916-0.4260 for PK-V, 0.2873-0.4197 for PKRO-V and 0.2831-0.4136 for PKRI-V.

There is some sudden increase – decrease in discharge coefficients of unvented PK Weir, between head to weir height values of 0.06-0.15. The discharge coefficient increases from 0.4055 at $H_t/P=0.06$ to 0.4581 at $H_t/P=0.08$, then slightly decreases to 0.4543 at $H_t/P=0.0974$ then drastically jumps to maximum 0.4959 at $H_t/P=0.1062$ and finally continues decreasing as H_t/P increasing.

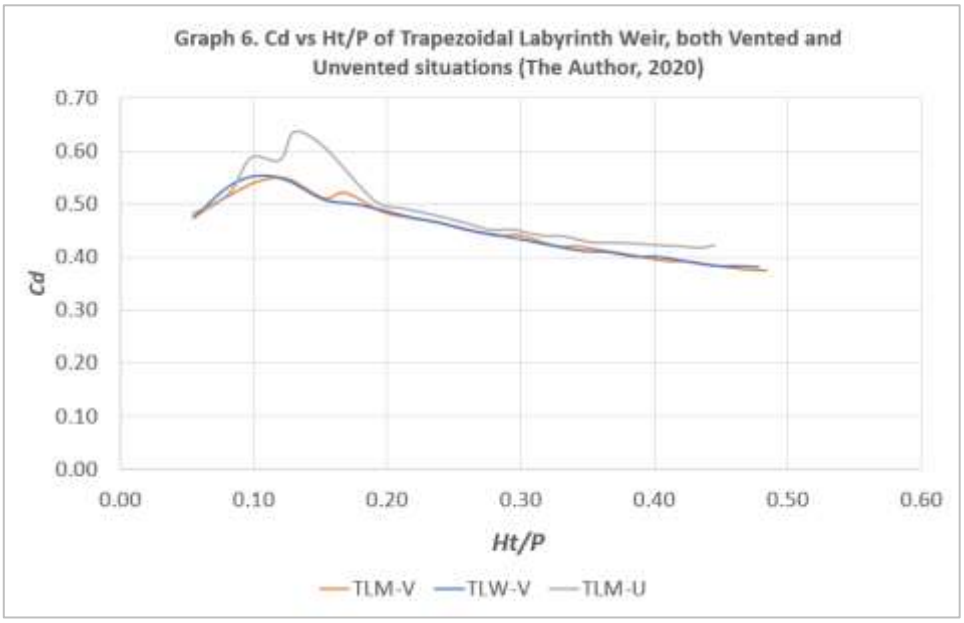

Graph 6. Discharge coefficient C_d versus head over weir height H_t/P of TL Weir, both vented and unvented situations

In Graph 6, it is seen that weir orientation has no effect on the discharge coefficient of TL Weir, both in vented and unvented situations. In general, TL Weir in unvented situations has slightly higher values of discharge coefficients with the same head to weir height values, compared to vented TL Weir situations.

The range of discharge coefficient of TL Weir in unvented situations are 0.4190-0.6374 for TLM-U, similar for inverse orientation. The range of discharge coefficient of TL Weir in vented situations are slightly lower, 0.3749-0.5476 for TLM-V and 0.3813-0.5538 for TLW-V.

A similar increase – decrease trend in discharge coefficients of unvented TL Weir, between head to weir height values of 0.08-0.18, is recognized. The discharge coefficient increases from 0.5212 at H_t/P=0.08 to 0.5888 at H_t/P=0.1, then slightly decreases to 0.5839 at H_t/P=0.1250 then drastically jumps to maximum 0.6374 at H_t/P=0.1304 and finally continues decreasing as Ht/P increasing.

5.2 Limitations of the Research

1. The pump capacity limited to only 21 l/s. Therefore, this experiment was repeated only 21 times and the central limit theory could not be done since it requires 30 samples.
2. The propeller flow meter provided, at times, unexpected velocity values downstream. However, this was solved by getting the propeller flow meter out of the flume and using of a cloth to clean the propeller and placing it back.

3. The same positions of the sensors for the entire measurement process could not be achieved since it was difficult to adjust them to their initial positions with the help of the software. Therefore, the new positions were used and recorded for each experiment.
4. The experiment was limited to two models only, one PK Weir and one TL Weir. If this study was undertaken again, PK Weirs with overhang cantilevers and other additional configurations should be considered.

5.3 **Comparison of this study with the found research**

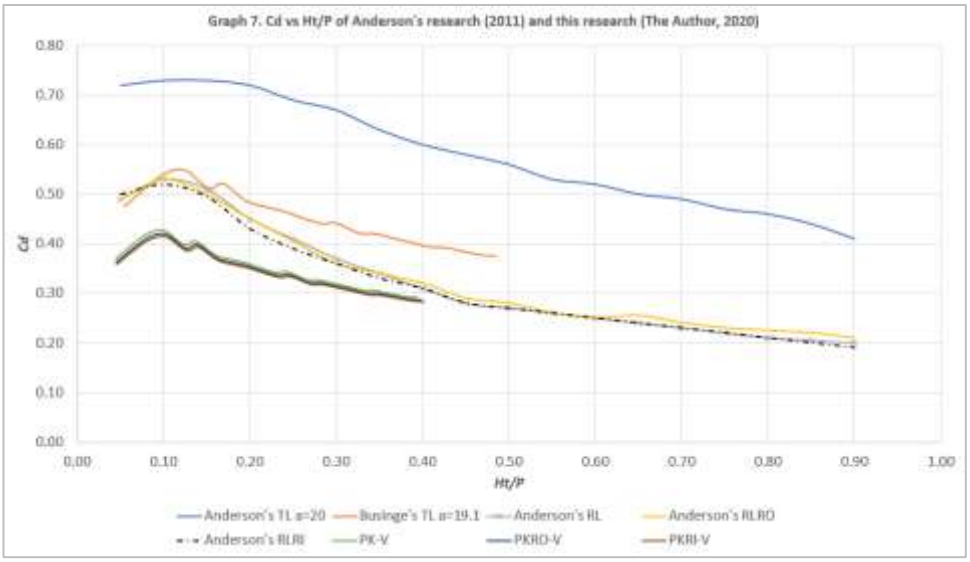

Graph 7. Discharge coefficient C_d versus head over weir height H_t/P of the found research from Anderson (2011) and this research

5.3.1 Similarities between Anderson's curves and this research's curves

- TL Weir has higher values of discharge coefficients compared to PK Weir for both experiments.
- PK Weir has higher discharge efficiency than TL Weir.

5.3.2 Differences between Anderson's curves and this research's curves

The research by Anderson (2011) has higher values of discharge coefficients and larger H_t/P range for both PK Weir and TL Weir than this research. This is attributed to the following reasons that already mentioned in chapter 2.3.2 above:

- The flume used by Anderson (2011) was 7.30 m long, 0.93 m wide, 0.60 m deep while in this research it was 10 m long, 0.30 m wide and 0.47 m deep.
- The research by Anderson (2011) used one pump capable of 240.70 l/s while this research used one pump with a capacity of 21 l/s.

- In the research by Anderson (2011), tests were run with flows ranging from 7.08 l/s to 240.70 l/s while in this research, the flows were from 1 l/s to 21 l/s.
- The PK Weirs in Anderson's research (2011) were designed as 4 cycles while in this research, the weirs are designed as 2 cycles.
- The Labyrinth Weirs in Anderson's research (2011) were designed as 4 cycles while in this research, the weirs are designed as 2 cycles.

5.4 **Summary of Chapter**

This chapter has explained the graphs of Discharge (Q) versus Water Level above the weir crest (H_t), the Discharge Coefficient (C_d) versus Head to Weir Height (H_t/P) for both vented and unvented situations for PK Weir and TL Weir. A comparison of results of the found research with this experiment was carried out.

6 **CONCLUSIONS**

The first chapter of this thesis introduced the background and the need to conduct a laboratory experiment to determine the Discharge Coefficient of a PK Weir and compare to that of a TL Weir.

To achieve this aim, the following objectives were pursued: understand the literature, methodology and findings of the previous study by Businge (2020), adapt the methodology for collecting hypothetical data, predict from the hypothetical data the Discharge Coefficient of a PK Weir and compare to the collected data from the laboratory experiment of a TL Weir, discuss the results of the analysis/comparison, ensure the next researcher will be able to conduct the actual laboratory experiment described in this study.

The second chapter presented the overview of previous literature, its place and publication, the methodology used, differences between the previous research and this research, weaknesses in the previous research that have been strengthened in this research and results of the previous research. Topics such as different types of PK Weirs, vented versus unvented overflow, effect of weir orientation on TL Weirs and cost comparison between PK Weir and TL Weir have been discussed.

The third chapter described the methodology adopted from the previous literature and the reasons why it has been adopted, description of the experimental setup and the experimental procedure.

The fourth chapter presented Tables of Predicted Results for PK Weir and Table of Results for TL Weir (Businge, 2020). That led to the plotting of the graphs of:

1. A graph of discharge versus water level for both PK Weir and TL Weir in vented situation (PK-V, PKRO-V, PKRI-V, TLM-V, TLW-V).
2. A graph of discharge versus water level for both PK Weir and TL Weir in unvented situation (PK-U, PKRO-U, PKRI-U, TLM-U, TLW-U).
3. A graph of discharge coefficient versus head over weir height for the vented situation (PK-V, PKRO-V, PKRI-V, TLM-V, TLW-V).
4. A graph of discharge coefficient versus head over weir height for the unvented situation (PK-U, PKRO-U, PKRI-U, TLM-U, TLW-U).
5. A graph of discharge coefficient versus head over weir height for PK Weir (PK-U, PKRO-U, PKRI-U, PK-V, PKRO-V, PKRI-V).
6. A graph of discharge coefficient versus head over weir height for the M-shape and W-shape TL Weir (TLM-U, TLW-U, TLM-V, TLW-V).

Finally, the fifth chapter explained the graphs of Discharge (Q) versus Water Level above the weir crest (H_t), the Discharge Coefficient (C_d) versus Head to Weir Height (H_t/P) for both vented and unvented situations for PK Weir and TL Weir. A comparison of results of the previous research with this experiment was carried out. Deductions were made from graph observations:

- TL Weir experiences higher water levels than PK Weir for the same discharges, under similar flow conditions, in both vented and unvented situations.
- The differences in water levels varies between the weirs, in both vented and unvented situations. However, in general, the differences in water levels between TL Weir and PK Weir in vented situations are slightly higher.
- There are little differences between different configurations of PK Weir (with or without ramps) and TL Weir (normal and inverse orientation), both in vented and unvented situations.
- With the same head over weir height H_t/P, in both vented and unvented situations, PK Weir experiences higher discharge Q with lower discharge coefficient C_d. PK Weir discharges, from 23% to 135% more than TL Weir.
- PK Weir has higher discharge efficiency than TL Weir with more length L can fit within the given fixed width W and breath B at a given value of H_t/P.
- The range of discharge coefficient of PK Weir in unvented situations are generally 0.3259-0.4959. The range of discharge coefficient of PK Weir in vented situations are lower, around 0.2916-0.4260.

- The range of discharge coefficient of TL Weir in unvented situations are generally 0.4190-0.6374. The range of discharge coefficient of TL Weir in vented situations are slightly lower, around 0.3749-0.5476.

RECOMMENDATION

In the future research, one could run the actual experiment of PK Weir based on the predicted data from this research and compare again with those data.

REFERENCES

Anderson, R. M. (2011). *Piano Key Weir Head Discharge Relationships*. Master's Thesis, Utah State University. Retrieved March 25, 2020, from https://digitalcommons.usu.edu/etd/880/.

Businge, P. E. (2020). *An Investigation into the Coefficient of Discharge of a Labyrinth Weir and Rehbock (Linear Weir)*. Bachelor Thesis, Mainz University of Applied Sciences. Retrieved March 25, 2020, from https://www.hs-mainz.de/en/.

Barcouda, M., Cazaillet, O., Cochet, P., Jones, B. A., Lacroix, S., Laugier, F., Odeyer, C., Vingny, J. P., (2006). *Cost-Effective Increase in Storage and Safety of Most Dams Using Fuse gates or P.K. Weirs*. Proc. of the 22nd Congress of ICOLD., Barcelona, Spain.

Chanson, H. (1999). *The Hydraulics of Open Channel Flow*. London: Arnold.

Engineering Notes (2020). *Classification or Types of Notches and Weirs in Fluid Mechanics*. Retrieved May 2, 2020, from https://www.engineeringenotes.com/fluids/weirs/classification-or-types-of-notches-and-weirs-fluid-mechanics/47397

General Acoustics (2017). *UltraLab ULS HF54/58*. Retrieved April 28, 2020, from https://www.generalacoustics.com/

Hillhouse, G. (2019). *What is a weir*. Retrieved March 25, 2020, from https://practical.engineering/blog/2019/3/9/what-is-a-weir.

Hanania, J., Stenhouse, K. and Donev, J. (2017). *Weir*. Retrieved March 25, 2020, from https://energyeducation.ca/encyclopedia/Weir.

Hamburg University of Technology (2020). *Weirs with free critical overflow*. Retrieved March 25, 2020, from http://daad.wb.tu-harburg.de/tutorial/flood-probability-assessment/hydrodynamics-of-floods/1d-hydrodynamic-models/theory/fundamentals-of-mathematical-river-flow-modelling-1d-water-level-calculation/hydraulic-structures/weirs/weirs-with-free-critical-overflow/

Idrees, A. K., Al-Ameri, R. and Das, S. (2016). Determination of Discharge Coefficient for flow over one cycle compound Trapezoidal Planform Labyrinth Weir. *International Journal of Civil Engineering and Technology, 7*(4), 314-328.

Lemperiere, F. and Ouamane, A. (2003). The Piano Keys weir: a new cost-effective solution for spillways. *The International Journal on Hydropower & Dams*, (5).

Machiels, O., Erpicum S., Archambeau, P., Dewals, B. and Pirotton, M. (2012). Parapet wall effect on Piano Key Weirs efficiency. *Journal of Irrigation and Drainage Engineering, 139(*6).

Open Channel Flow (2020). Aerations of weir nappes. Retrieved March 25, 2020, from https://www.openchannelflow.com/blog/aeration-of-weir-nappes.

Ouamane, A., Lempérière, F., (2006). *Design of a new economic shape of weir*. Proc. of the International Symposium of Dams in the Societies of the 21st Century, Barcelona, Spain, 463-470.

Ribeiro, M. L., Boillat, J. L., Schleiss, A., Laugier, F., Albalat, C. (2007). *Rehabilitation of St-Marc dam – Experimental Optimization of a Piano Key Weir*. Proc. of 32nd Congress of IAHR., Vince, Italy.

Ribeiro, M. L., Bieri, M., Boillat, J. L., Schleiss, A. J., Delorme, F., Laugier, F. (2009). *Hydraulic capacity improvement of existing spillways – Design of Piano Key weirs*. Proc. of 23rd Congress of ICOLD., Brasilia, Brazil.

Schleiss, A. J. (2011). From Labyrinth to Piano Key Weirs – A historical review. *Labyrinth and Piano Key Weirs – PKW 2011*, 3-15.

Schnabel Engineering. Lake Townsend Dam. Retrieved March 25, 2020, from https://www.schnabel-eng.com/blog/project/lake-townsend-dam/.

Paxson, G. S., Tullis, B. P. and Hertel D. J. (2014). *Comparison of Piano Key Weirs with labyrinth and gated spillways: Hydraulics, cost, constructability, and operations*. Retrieved March 25, 2020, from https://www.researchgate.net/publication/290525667_Comparison_of_piano_keyweirs_with_labyrinth_and_gated_spillways_Hydraulics_cost_constructability_and_operations.

Peter, G. (2014). *The discharge and run off calculation of weirs under the consideration of dynamic flows*. Retrieved March 25, 2020, from http://www.gelogmbh.de/downloads/1996artikelengl.pdf.

Truong, C. H., Ho, T. K. M & Dinh, S. Q. (2006). *Results of some piano keys weir hydraulic model tests in Vietnam*. Proc. of the 22nd Congress of ICOLD. Barcelona, Spain.

Universal Flow Monitors (2020). *Propeller Flow Meter Technology*. Retrieved April 28, 2020, from https://www.flowmeters.com/product-list.php?page=propeller-technology/pg1-cid97.html=/asc_action=SetCurrCat/category_id=97.

Universal Flow Monitors (2020). *Magnetic Flow Meter Technology*. Retrieved April 28, 2020, from https://www.flowmeters.com/product-

list.php?page=magnetic-technology/pg1-cid95.html=/asc_action=SetCurrCat/category_id=95.

Young, N. L. (2018). Size-Scale Effects of Nonlinear Weir Hydraulics. Master's Thesis, Utah State University. Retrieved March 25, 2020, from https://digitalcommons.usu.edu/etd/6926/.